AD_____

Award Number: W81XWH-09-1-0174

TITLE: Does the Altered Expression of Ion Channels Give Rise to the Enhanced Excitability of Neurons Isolated from Nf1 +/- Mice?

PRINCIPAL INVESTIGATOR: Grant Nicol

CONTRACTING ORGANIZATION: Indiana University School of Medicine
Indianapolis, IN 46202

REPORT DATE: September 2011

TYPE OF REPORT: Final

PREPARED FOR: U.S. Army Medical Research and Materiel Command
Fort Detrick, Maryland 21702-5012

DISTRIBUTION STATEMENT: Approved for Public Release;
Distribution Unlimited

The views, opinions and/or findings contained in this report are those of the author(s) and should not be construed as an official Department of the Army position, policy or decision unless so designated by other documentation.

# REPORT DOCUMENTATION PAGE

*Form Approved*
*OMB No. 0704-0188*

Public reporting burden for this collection of information is estimated to average 1 hour per response, including the time for reviewing instructions, searching existing data sources, gathering and maintaining the data needed, and completing and reviewing this collection of information. Send comments regarding this burden estimate or any other aspect of this collection of information, including suggestions for reducing this burden to Department of Defense, Washington Headquarters Services, Directorate for Information Operations and Reports (0704-0188), 1215 Jefferson Davis Highway, Suite 1204, Arlington, VA 22202-4302. Respondents should be aware that notwithstanding any other provision of law, no person shall be subject to any penalty for failing to comply with a collection of information if it does not display a currently valid OMB control number. **PLEASE DO NOT RETURN YOUR FORM TO THE ABOVE ADDRESS.**

| 1. REPORT DATE | 2. REPORT TYPE | 3. DATES COVERED |
|---|---|---|
| 01-09-2011 | Final | 1 September 2009 – 31 August 2011 |

**4. TITLE AND SUBTITLE**

Does the Altered Expression of Ion Channels Give Rise to the Enhanced Excitability of Neurons Isolated from Nf1 +/- Mice?

**5a. CONTRACT NUMBER**

**5b. GRANT NUMBER**
W81XWH-09-1-0174

**5c. PROGRAM ELEMENT NUMBER**

**6. AUTHOR(S)**

Grant Nicol

**E-Mail:** gnicol@iupui.edu

**5d. PROJECT NUMBER**

**5e. TASK NUMBER**

**5f. WORK UNIT NUMBER**

**7. PERFORMING ORGANIZATION NAME(S) AND ADDRESS(ES)**

Indiana University School of Medicine
Indianapolis, IN 46202

**8. PERFORMING ORGANIZATION REPORT NUMBER**

**9. SPONSORING / MONITORING AGENCY NAME(S) AND ADDRESS(ES)**
U.S. Army Medical Research and Materiel Command
Fort Detrick, Maryland 21702-5012

**10. SPONSOR/MONITOR'S ACRONYM(S)**

**11. SPONSOR/MONITOR'S REPORT NUMBER(S)**

**12. DISTRIBUTION / AVAILABILITY STATEMENT**
Approved for Public Release; Distribution Unlimited

**13. SUPPLEMENTARY NOTES**

**14. ABSTRACT**
We reported previously that sensory neurons isolated from mice with a heterozygous mutation of the Nf1 gene (Nf1+/-) exhibited greater excitability and increased sodium current densities compared to wildtype mice. This raises the question as to whether the increased current density resulted from post-translational modifications or increased expression of sodium channels. Quantitative real-time PCR was used to measure expression levels of the nine different voltage-gated sodium channel α subunits and the four associated auxiliary β subunits in the dorsal root ganglia (DRG) obtained from wildtype and Nf1+/- mice. The Relative Expression Software Tool indicated that Nav1.1, Nav1.3, Nav1.7, and Nav1.8 were significantly elevated in DRG isolated from Nf1+/- mice. Expression of Nav1.2, Nav1.5, Nav1.6, and Nav1.9 were not significantly altered. The gene transcript for Nav1.4 was not detected. There were no significant changes in the relative expression levels of beta subunits. The Nav1.9 subtype was the most abundant with Nav1.7 and Nav1.8 being the next most abundant subtypes, whereas Nav1.3 was relatively less abundant. For the beta subunits, B1 was by far the most abundant subtype. These results demonstrate that the increased expression levels of Nav1.7, Nav1.8, and perhaps Nav1.1 in the Nf1+/- DRG make the largest contribution to the increased sodium current density and thus give rise to the enhanced excitability.

**15. SUBJECT TERMS**
Neurofibromatosis, enhanced pain sensitivity, sodium channel expression

| 16. SECURITY CLASSIFICATION OF: | | | 17. LIMITATION OF ABSTRACT | 18. NUMBER OF PAGES | 19a. NAME OF RESPONSIBLE PERSON |
|---|---|---|---|---|---|
| a. REPORT | b. ABSTRACT | c. THIS PAGE | | | USAMRMC |
| U | U | U | UU | 20 | 19b. TELEPHONE NUMBER *(include area code)* |

**Table of Contents**


| | Page |
|---|---|
| **Introduction……..** | **1** |
| **Body……..** | **2-7** |
| **Key Research Accomplishments……..** | **7** |
| **Reportable Outcomes……** | **7** |
| **Conclusion……** | **8** |
| **References……** | **8-10** |
| **Appendices……** | **10** |


INTRODUCTION:

Neurofibromatosis type 1 (NF1) is an autosomal dominant disorder with an incidence of 1 in 3,000 people and is characterized by numerous abnormalities that include benign neurofibromas, malignant peripheral tumors of the nerve sheath, astrocytomas, bone deformities, and myeloid leukemias (Friedman, 1999). Some people with NF1 experience greater intensities of painful sensations to different stimuli, such as minor injuries, than those without this genetic disorder (Creange et al., 1999; Wolkenstein et al., 2001). NF1 is a consequence of a heterozygous mutation of the gene that encodes the protein, neurofibromin (*NF1*+/-). Neurofibromin is richly expressed in the nervous system (Datson et al., 1992) and promotes hydrolysis of Ras (Ras-GTP) to its inactive form (Ras-GDP) by serving as a GTPase activating protein (GAP). Mutations of *NF1* or the mouse ortholog *Nf1*, frequently result in enhanced basal and cytokine-stimulated Ras activity in many cell types, including sensory neurons (Largaespada et al., 1995; Vogel et al., 1995; Zhang et al., 1998; Lau et al., 2000). Increased Ras activity may influence protein expression levels. For example, expression of a GAP-resistant Ras in AtT20 cells induced expression of a potassium channel that greatly shortened the duration of the action potential and led to repetitive action potential firing (Hemmick et al., 1992). Similarly, Ras transformation of a fibroblast cell line lead to the expression of a $Ca^{2+}$-dependent potassium current that was not detected in non-transformed cells (Rane, 1991). These studies suggest that the heterozygous deletion of neurofibromin and altered Ras signaling can play a critical role in regulating the expression of ion channels that set the level of neuronal excitability.

We reported previously that small diameter, capsaicin-sensitive sensory neurons isolated from *Nf1*+/- mice exhibited augmented excitability (Wang et al., 2005) and that this enhanced excitability was likely the result of increased sodium current densities (Wang et al., 2010). Voltage-dependent sodium currents are critical in producing the upstroke of the action potential, which is the key component of neural communication. Molecularly, the alpha subunits of mammalian sodium channels have been categorized into one family consisting of nine different subtypes (Nav1.1-Nav1.9)(Goldin, 2001; Catterall et al., 2005). Pharmacologically, sodium channels have been classified according to their sensitivity to the blocker tetrodotoxin (TTX) wherein the currents conducted by Nav1.1-1.4, 1.6, and 1.7 are completely blocked whereas the currents carried by Nav1.5, Nav1.8, and Nav1.9 are resistant or insensitive to inhibition by the toxin. The TTX-sensitive sodium currents exhibit both rapid activation and inactivation properties whereas the TTX-resistant subtypes activate and inactivate more slowly. The properties of these different subtypes of sodium channels have been reviewed recently (Goldin, 2001; Catterall et al., 2005; Dib-Hajj et al., 2010). Associated with the alpha subunits are the modulatory beta subunits, of which four different subtypes exist (B1-B4). The beta subunits modulate the amplitude and kinetics of the currents conducted by the alpha subunits and also influence the trafficking and expression of the alpha subunits (reviewed by Isom, 2001; Patino and Isom, 2010). To determine the possible mechanisms giving rise to the augmented neuronal firing and sodium current density in *Nf1*+/- sensory neurons, the relative expression levels of mRNA for the α subtypes and beta subunits of voltage-gated sodium channels were determined in wildtype and *Nf1+/-* neurons of the dorsal root ganglion (DRG). Consistent with our physiological observations, DRG obtained from *Nf1+/-* mice exhibited increased levels for some but not all α subunits while the beta subunits were not altered.

BODY:

Our previous studies indicated that sensory neurons isolated from *Nf1+/-* mice exhibited increased excitability that resulted from elevated levels of voltage-dependent sodium currents (Wang et al., 2005; 2010). To determine if the augmented sodium currents were a consequence of increased expression of sodium channel mRNA, quantitative PCR was performed using DRG isolated from wildtype and *Nf1+/-* mice. The average Cq values obtained for eight of the nine different voltage-dependent α subunits and the four auxiliary β subunits are summarized in Table 3. The Cq values indicate that in wildtype mice Nav1.9 (23.63 ± 0.34, n=5 mice) was the most abundant channel subtype with Nav1.7 (26.58 ± 0.53, n=7 mice) and Nav1.8 (26.30 ± 0.43, n=7 mice) being the next most abundant subtypes whereas Nav1.3 was less abundant (33.07 ± 0.62, n=7 mice). For the β subunits, β1 was by far the most abundant subtype and β2 the least abundant. The gene transcripts for Nav1.4 were not detected in the DRG, consistent with previous observations that the expression of Nav1.4 is limited to skeletal muscle (Trimmer et al., 1989). The primers used in our study were capable of detecting Nav1.4 in mRNA isolated from mouse skeletal muscle (Cq = 26.25 ± 0.05, data not shown).

**Table 3.** Cq values

| Gene | Wildtype | Nf1+/– |
|---|---|---|
| Nav1.1 | 27.44±0.48 | *26.95±0.10* |
| Nav1.2 | 31.38±0.37 | *31.07±0.13* |
| Nav1.3 | 33.07±0.62 | *32.32±0.09* |
| Nav1.5 | 31.71±0.45 | *31.24±0.20* |
| Nav1.6 | 27.54±0.44 | *27.12±0.26* |
| Nav1.7 | 26.58±0.53 | *25.94±0.14* |
| Nav1.8 | 26.30±0.43 | *25.83±0.19* |
| Nav1.9 | 23.63±0.34 | *23.93±0.15* |
| *β*1 | 24.37±0.26 | *24.55±0.15* |
| *β*2 | 28.37±0.34 | *28.24±0.17* |
| *β*3 | 26.75±0.28 | *26.95±0.08* |
| *β*4 | 26.48±0.33 | *26.34±0.24* |
| HPRT | 24.79±0.29 | *24.66±0.20* |
| *Arbp* | *21.36±0.12* | *21.31±0.19* |

Values of Nav1.1–1.8, HPRT, Arbp represent means±SEM *n*=7 and 6 for wildtype and *Nf1+/–*, respectively; for Nav1.9 *n*=5 of each genotype and for *β*1–*β*4 *n*=4 of each genotype.

To assess whether there were differences in the mRNA levels for these sodium channels between the two genotypes, the expression of sodium channel subtypes was normalized to two reference genes, HPRT and Arbp. The relative differences in channel expression were determined by using a method described by Pfaffl (2001) wherein the Cq values are corrected by accounting for the efficiency of the PCR for both the targeted and reference genes. The relative expression for the α subunits of sodium channel subtypes determined in the *Nf1+/-* mice compared to the wildtype is summarized in Fig. 1A. An analysis using the REST protocol indicated that Nav1.1 (1.67-fold), Nav1.3 (2.04-fold), Nav1.7 (1.87-fold), and Nav1.8 (1.48-fold) were elevated significantly (P<0.05) in the DRG isolated from *Nf1+/-* mice compared to the wildtype. The expression of Nav1.2 (1.27-fold), Nav1.5 (1.52-fold), Nav1.6 (1.42-fold), and Nav1.9 (0.65-fold) were not significantly altered. In addition, as summarized in Fig. 1B, there were no significant differences in the relative expression of β subunits. These results demonstrate that the expression of some sodium channel subtypes is increased in *Nf1+/-* mice and therefore could account for the elevated excitability and sodium current densities recorded from *Nf1+/-* neurons.

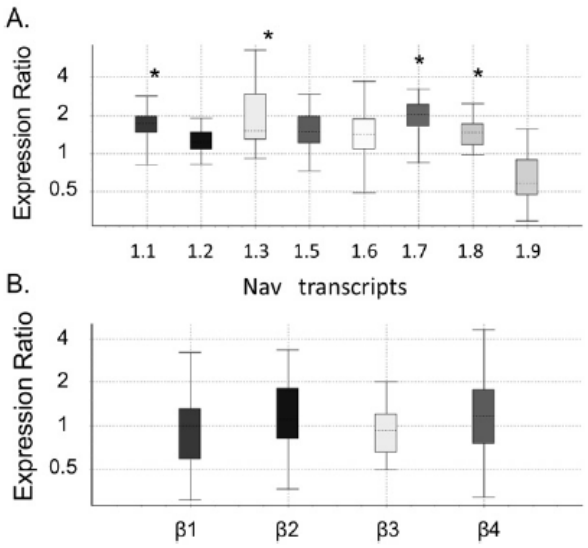


**Fig. 1.** mRNA expression of some sodium channel subtypes is elevated in the DRG of *Nf1+/–* mice compared with wildtype mice. Panel (A) represents the relative expression levels for eight of the nine sodium channel subtypes relative to the reference genes HPRT and Arbp obtained with the REST analysis protocol. The expression of Nav1.1, Nav1.3, Nav1.7, and Nav1.8 were significantly increased (*P*<0.05) in the *Nf1+/–*DRG compared with the wildtype DRG. Panel (B) illustrates the relative expression levels for the auxiliary *β* subunits relative to HPRT and Arbp. The asterisks indicate a statistical difference (*P*<0.05) using the Relative Expression Software Tool (REST, 2009).

This observation raises the question as to whether there are changes in the contribution of individual sodium channel subtypes to the total mRNA pool in these genotypes that could account for the elevated sodium current densities in the *Nf1+/-* sensory neurons. The fractional contribution of each channel subtype to the total mRNA copy number is illustrated in Fig. 2. The results were obtained from four mice of each genotype wherein qPCR was performed for Nav1.1-Nav1.9 and β1-β4. The copy number ($Eff^{-Cq}$) for each channel was calculated and the total value was determined

for each mouse. The average copy number for each channel subtype was determined for the four mice of each genotype. The fractional contribution of each channel subtype was then assessed by dividing the average copy number for each channel by the average total. Overall, there was not a significant difference between the genotypes in the fractional contribution of a particular channel subtype to the total sodium channel mRNA (Fig. 2A). However, based on the average values, there is a trend towards higher fractional levels of Nav1.6, Nav1.7, and Nav1.8 in the *Nf1+/-* DRG compared to the wildtype. The largest contributors to the total mRNA were the TTX-resistant sodium channels Nav1.9 (42.9 and 43.1% in the wildtype and *Nf1+/-* neurons, respectively) and Nav1.8 (16.0 and 21.3% in the wildtype and *Nf1+/-* neurons, respectively). Of the TTX-sensitive sodium channels Nav1.6 (8.1 and 10.8% in the wildtype and *Nf1+/-* neurons, respectively) and Nav1.7 (11.2 and 15.3% in the wildtype and *Nf1+/-* neurons, respectively) made the largest contribution. Nav1.2, Nav1.3, and Nav1.5 made only a small contribution (<1%) and are shown in the inset of Fig. 2A. Of the β subunits, β1 comprised more than 60% of the total mRNA for these auxiliary subunits in both wildtype and *Nf1+/-* sensory neurons (see Fig. 2B). There is a trend towards a higher fractional contribution of β1 in the *Nf1+/-* DRG (68.3%) compared to the wildtype DRG (62.3%) and a lower fractional contribution of β4 in the *Nf1+/-* DRG (15.4%) compared to the wildtype DRG (24.9%). Therefore, these results demonstrate that despite an increase in the overall expression of Nav1.1, Nav1.3, Nav1.7 and Nav1.8, the patterns of predominance remain similar between genotypes. This supports the change in excitability that we have observed previously (Wang et al., 2005; 2010), but suggests that a change in the phenotype of the sensory neuron, for example to a more TTX-sensitive form, does not occur.

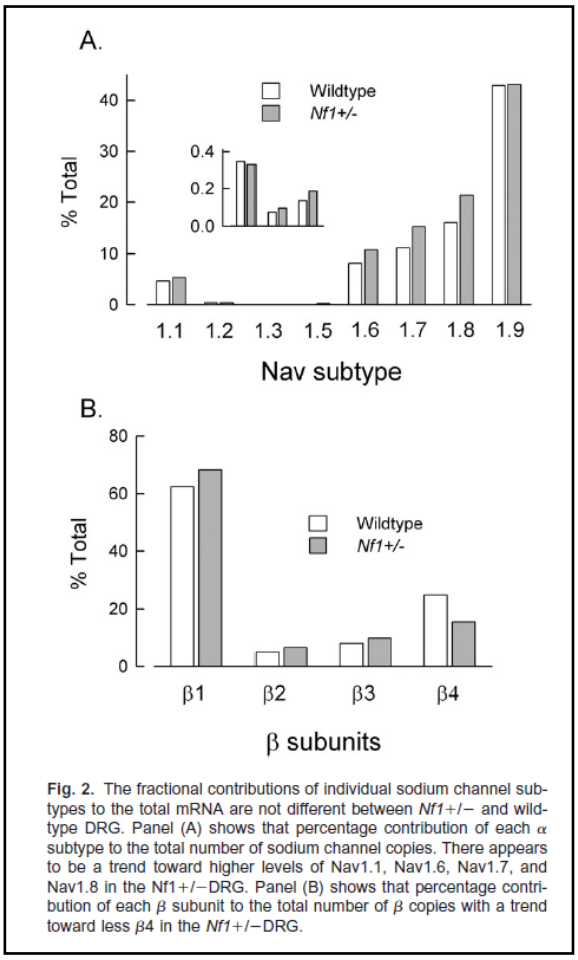


**Fig. 2.** The fractional contributions of individual sodium channel subtypes to the total mRNA are not different between *Nf1+/−* and wildtype DRG. Panel (A) shows that percentage contribution of each α subtype to the total number of sodium channel copies. There appears to be a trend toward higher levels of Nav1.1, Nav1.6, Nav1.7, and Nav1.8 in the Nf1+/−DRG. Panel (B) shows that percentage contribution of each β subunit to the total number of β copies with a trend toward less β4 in the *Nf1+/−*DRG.

The results reported here indicate that expression of the sodium channel subtypes Nav1.1, Nav1.3, Nav1.7, and Nav1.8 were elevated significantly in the DRG isolated from *Nf1+/-* mice compared to wildtype mice. Similar values for the increases in these channel subtypes were observed using either reference gene, HPRT or Arbp, indicating the stability of these genes for the normalization of channel expression. The elevated levels of sodium channel mRNA are consistent with our previous reports that sensory neurons isolated from the DRG of *Nf1+/-* mice generated two-fold more action potentials in response to the same level of current stimulation (Wang et al., 2005) and that the sodium current density for both TTX-sensitive and TTX-resistant currents was significantly elevated in the *Nf1+/-* sensory neurons (Wang et al., 2010). Furthermore, expression levels of the β subunits were measured as these subunits modulate the amplitude and kinetics of the currents conducted by the α subunits and can also influence the trafficking and surface density of the α subunits (reviewed by Isom, 2001; Patino and Isom, 2010). However, there were no differences in the expression levels of the auxiliary β subunits between the two genotypes suggesting that altered β subunit expression does not contribute to the increased sodium current densities in *Nf1+/-* sensory neurons.

The neurons of the DRG are a heterogeneous population and are activated by a variety of sensory modalities. The reader is referred to the following reviews regarding expression, biophysical properties, and physiological impact of voltage-dependent sodium channels (Black et al., 1996; Catterall et al., 2005; Rush et al., 2007; Cummins et al., 2007; Fukuoka et al., 2008; Docherty and Farmer, 2009; Dib-Hajj et al., 2010). Generally speaking, these neurons are classified into three groups based on cell body diameter and their corresponding conduction velocities (Harper and Lawson, 1985a/b; Lawson, 2002). Small diameter neurons (<25 μm) give rise to unmyelinated C-fibers which have slow conduction velocities (<1.4 m/s), medium diameter neurons (25-40 μm) give rise to lightly myelinated Aδ fibers having faster conduction velocities (2-8 m/s), and large diameter (>40 μm) give rise to more heavily myelinated Aα/β fibers that have conduction velocities >14 m/s (Harper and Lawson, 1985a/b; Lawson, 2002). Previous studies (Black et al., 1996; Cummins et al., 2007; Fukuoka et al., 2008; Docherty and Farmer, 2009; Dib-Hajj et al., 2010) have shown that sensory

neurons in the rat DRG express the TTX-sensitive sodium channels Nav1.1, Nav1.2, Nav1.3, Nav1.6, and Nav1.7 as well as the TTX-resistant channels Nav1.5, Nav1.8, and Nav1.9. Nav1.1 and Nav1.6 are preferentially expressed in large diameter (>50 μm) sensory neurons although these subtypes are expressed at low levels in small and medium diameter sensory neurons. Nav1.2 and Nav1.5 appear to be expressed at low levels in nociceptive small diameter (<25 μm) sensory neurons. The small diameter neurons are of particular interest as they are often the predominant cell type involved in painful or nociceptive signaling. It is important to consider that some portion of the total expression for individual sodium channel subtypes may be contributed from glia localized in DRG as previous studies have documented expression of sodium channels in both astrocytes and microglia (Bevan et al., 1985; Waxman et al., 1993; Black et al., 2009; 2010).

Our observations are consistent with recent reports examining the expression of sodium channel subtypes in rat sensory neurons. Using mRNA isolated from rat L4/5 DRG, Berta et al. (2008) found that Nav1.7 was the most abundant transcript, Nav1.8 and Nav1.6 were about half the levels of Nav1.7 and Nav1.1 was slightly less than Nav1.6. The levels of Nav1.2, Nav1.3, and Nav1.9 were much lower and Nav1.5 was undetected. For the β subunits, β1 and β4 were about equal while β3 and β2 were much less expressed. The expression profiles of Nav1.9 and the β subunits are different than what we report in mouse sensory neurons, however, we obtained mRNA from L4/5 as well as more rostral DRG. In sensory neurons isolated from the L4/5 DRG of adult rats and grown in culture for <30 hr, Nav1.7 exhibited the highest level of expression with Nav1.8 and Nav1.1 being the next most abundant, Nav1.2, Nav1.3, and Nav1.6 were substantially less (Wang et al., 2008). The level of Nav1.9 was quite low in the isolated neurons although Nav1.9 was comparable to Nav1.8 in the intact whole DRG, which is in contrast to the findings reported by Berta et al. Nav1.4 and Nav1.5 were not detected by these authors. In electrophysiologically characterized rat sensory neurons that underwent single cell qPCR (Ho and O'Leary, 2011), Nav1.7, Nav1.8, and Nav1.9 were the most prominently expressed subtypes in small diameter (<25 μm) sensory neurons although Nav1.1, Nav1.2, and Nav1.6 were detected at lower levels. In large diameter (>30 μm) neurons, Nav1.7 was the most abundant followed by Nav1.6 and Nav1.1, with only low levels of Nav1.2 and Nav1.9 detected. A surprisingly high expression of Nav1.8 was exhibited by a subpopulation of large neurons. Nav1.5 was detected in approximately 14% of the neurons examined (Ho and O'Leary, 2011). In contrast to findings obtained in rat DRG, we found that the fractional expression of Nav1.9 was the highest of all the α subunits in the mouse DRG. Previous results indicated that Nav1.9 was expressed in only ~50% of rat unmyelinated C-fibers (Amaya et al., 2000; Fukuoka et al., 2008). However, using the average number of mRNA copies measured in single sensory neurons isolated from rat DRG as reported by Ho and O'Leary (2011), the fractional expression of Nav1.9 in small diameter (<25 μm) neurons was ~35% of the total (n=70 neurons) whereas in the large diameter (>30 μm) it was only ~5% (n=69 neurons) (O'Leary, personal comm.). In addition, in whole isolated rat ganglia, Nav1.9 comprised ~28 ± 2% of the total mRNA (n=4 ganglia) and is similar to our value for Nav1.9 making up ~40% of the total mRNA (O'Leary, personal comm.). The exact origins for the differences reported in the literature are presently unknown. To our knowledge, our study is the first to quantitatively determine the expression levels for Nav subunits in mouse DRG, hence one possibility for the larger expression of Nav1.9 mRNA is a species difference between rat and mouse. It is also possible that in the mouse DRG there may be large amounts of Nav1.9 mRNA held in reserve for translational upon metabolic demands or after neuronal injury. This is a subject for further investigation.

Nav1.7 is the predominant TTX-sensitive sodium channel expressed in small diameter neurons where it may play an important role in action potential firing The slowly developing inactivation properties of Nav1.7 promote action potential generation in response to slow depolarizing stimuli (Cummins et al., 1998). Therefore, it is likely that the near 2-fold increase in Nav1.7 expression seen in the *Nf1+/-* neurons would play a significant role in mediating the increased sodium current density and increased excitability that we have observed in the *Nf1+/-* sensory neurons compared to those from wildtype mice (Wang et al., 2005; 2010). Although Nav1.7 appears to be the highest expressed TTX-sensitive α subunit based on mRNA levels in small diameter sensory neurons, the amplitude of compound action potentials measured from sciatic C-fibers in Scn8med mice (Nav1.6 knock-out) was diminished, suggesting that Nav1.6 does contribute to action potential generation in these unmyelinated fibers (Black et al., 2002). Nav1.8 and Nav1.9 are the predominant TTX-resistant channels in small diameter neurons wherein Nav1.8 is thought to contribute to setting the firing threshold and regulating the upstroke of the action potential (Renganathan et al., 2001; Blair and Bean, 2002) whereas Nav1.9 may give rise to a persistent sodium current that influences excitability as well as in setting the resting membrane potential (Cummins et al., 1999; Herzog et al., 2001; Baker et al., 2003). However, at the normal resting potential of sensory neurons (around -60 mV), Nav1.9 is 97% inactivated by ultra-slow inactivation such that this channel

subtype may contribute little, if any, to the normal excitability of these neurons (Cummins et al., 1999). Of the TTX-resistant channels in sensory neurons, expression of Nav1.8 was significantly elevated in the *Nf1+/-* DRG compared to wildtype, suggesting that an increase in this channel is responsible for a component of the increased excitability of *Nf1+/-* sensory neurons at resting membrane potentials. TTX-resistant subtypes have been detected in large diameter neurons, however, the functional role of these channels in the physiological response of large diameter neurons is not presently understood. Interestingly, Nav1.3 is expressed in embryonic sensory neurons and then in adulthood this subtype is greatly diminished (Waxman et al., 1994; Dib-Hajj et al., 1996; Felts et al., 1997). After nerve injury Nav1.3 is re-expressed and may contribute to the increased excitability observed after injury (Cummins and Waxman, 1997; Cummins et al., 2001). Based on this, it is possible that the enhanced excitability and TTX-sensitive sodium current density observed in *Nf1+/-* sensory neurons could result from the increased expression of Nav1.3, however, this seems unlikely because Nav1.3 makes up only a small fraction of the total complement of sodium channel (Fig. 2A). Whereas the significant increases in the dominant channels, Nav1.7 and 1.8, are much more likely to be driving the changes in sodium current densities and excitability observed in *Nf1+/-* sensory neurons. Since gain of function mutations or increased expression of Nav1.7 or increased expression of Nav1.8 are associated with increased pain in humans (Jarecki et al., 2008; 2010; Cregg et al., 2010; Dib-Hajj et al., 2010,), increases in the expression of these channels in those with NF1 may play a role in the increased intensity of sensory symptoms experienced by some with this disorder. The causal mechanisms that give rise to changes in sodium channel gene expression in the context of reduced neurofibromin and the corresponding chronic enhancement of Ras activity are unexplored. Acute inhibition of Ras activation by the Ras blocking antibody, Y13-259, did not restore the increased excitability of *Nf1+/-* sensory neurons (Duan et al., 2011) back to levels observed in wildtype sensory neurons. This result indicates that it is the long-term reduction in neurofibromin, through increased Ras signaling, that is responsible for the increased sodium channel expression and excitability in *Nf1+/-* sensory neurons. As inhibition of Ras did recapitulate the lower levels of neuronal excitability observed in wildtype neurons, this would suggest that acute post-translational modifications of Nav do not contribute to the increased sodium current densities, however it is possible that other cellular mechanisms downstream of Ras may regulate membrane currents. These potential mechanisms remain an area of active investigation. Although the origins by which NF1 causes enhanced painful sensation have not been elucidated, it is likely that these abnormal painful states involve the sensitization of small diameter nociceptive sensory neurons and may underlie the onset of enhanced painful sensation in people with NF1.

In conclusion, in the DRG isolated from wildtype mice, the Nav1.9 subtype was the most abundant with Nav1.7 and Nav1.8 being the next most abundant subtypes. For the auxiliary β subunits, β1 was by far the most abundant subtype. The mRNA for the □subunits of the sodium channels Nav1.1, Nav1.3, Nav1.7, and Nav1.8 were significantly elevated in DRG isolated from *Nf1+/-* mice. There were no significant changes in the relative expression levels of the auxiliary β subunits. These results suggest that increased expression levels of Nav1.7, Nav1.8, and perhaps Nav1.1 in the *Nf1+/-* DRG make the largest contribution to the increased sodium current density and thus give rise to the enhanced excitability.

**Experimental Procedures**

*Animals*

Mice heterozygous for the *Nf1* mutation on a background of C57BL/6J were originally developed by Dr. Tyler Jacks (Jacks et al., 1994). All animals were housed, bred, and had free access to food and water in the Indiana University Laboratory Animal Research Center and were used in accordance with National Institute of Health Guide for Care and Use of Laboratory Animals (National Institutes of Health Publications No. 80–23, revised 1996). All procedures were approved by the Animal Use and Care Committee of the Indiana University School of Medicine.

*Isolation of the dorsal root ganglia*

The dorsal root ganglia (DRG) were isolated from young adult C57BL6J mice (2 to 3 months old). The wildtype and *Nf1+/-* mice used in these studies were littermates. Briefly, mice were killed by placing them in a $CO_2$ chamber and the spinal column was removed. Lumbar, cervical and thoracic DRG were collected and trimmed in cold, sterilized Puck's solution composed of (in mM): 171 NaCl, 6.7 KCl, 1.6 $Na_2PO_4$, 0.5 $KH_2PO_4$, 6 d-glucose, and 0.01% phenol red, pH 7.3. The ganglia were then transferred to a conical tube and washed with sterilized PBS. Tissues were stored at -80$^{o}$ C and used within two weeks.

*Real-Time quantitative PCR*

Total RNA was extracted from DRG tissue using the RNeasy® Plus Minikit (Qiagen, Valencia, CA) and assessed on a NanoDrop ND-1000 Spectrophotometer (Thermoscientific, Franklin, MA) for concentration ($A_{260}$) and purity by OD ratios ($A_{260}/A_{280}$, ranging between 2.0-2.2). Following treatment with DNase I (Invitrogen, Carlsbad, CA) to eliminate any residual genomic DNA, 1 µg RNA was reversed transcribed using the iScript cDNA Synthesis Kit (Bio-Rad, Hercules, CA) in 20 µl reactions according to the manufacturer's instructions. To assess the specificity of these reactions, no reverse transcriptase (RT) and no template controls were also generated. cDNA was stored at -20°C prior to PCR detection. Reverse transcription products were diluted and amplified in 25 µl reactions using Power SYBR® Green PCR Master Mix (Applied Biosystems, Carlsbad, CA) and 500 nM forward and reverse primers (Invitrogen). Sodium channel primers were designed specifically against mouse transcripts using PrimerExpress® software v3.0 (Applied Biosystems) and were based on a previous publication (Wang et al., 2008) describing PCR amplification of mRNA for voltage-dependent sodium channels in rat DRG. Hypoxanthine-guanine phosphoribosyl transferase (HPRT) and acidic ribosomal protein P0 (Arbp) were selected as reference genes for normalization of the quantitative PCR (qPCR) results. The accession number(s), amplicon size and position, and primer sequences for all genes targeted in this study are shown in Table 1. Primers were initially tested in tissues known to express the targeted sodium channel subtype, for example Nav1.4 was detected in

**Table 1.** Primer sequences

| Gene | Accession no. | Prod (bp) | Pos | *Seq (5′–3′)* |
|---|---|---|---|---|
| Nav1.1 | NM_018733.2 | 123 | 4465..4587 | *f-CATGTATGCTGCAGTTGATTCCA*<br>*r-AACAGGTTCAGGGTAAAGAAGG* |
| Nav1.2 | NM_001099298.2 | 82 | 2992..3073 | *GCCTTGCTCCTCAGTTCTTTCA*<br>*CGGCTATCTGGAGGTTGTTCA* |
| Nav1.3 | NM_018732.3 | 95 | 4153..4247 | *GGTGTGCCTCATCTTCTGGTTAA*<br>*TGCTGCCCGTTGTCATGTTA* |
| Nav1.4 | NM_133199.2 | 94 | 391..484 | *CGCGCTGTTCAGCATGTT*<br>*CTCCACGTCCTTGGACCAAG* |
| Nav1.5 | NM_021544.3 | 83 | 1142..1224 | *ACCTCAATGACCCAGCCAATTA*<br>*TGTCCCGGCATCAGAGCT* |
| Nav1.6 | NM_001077499.1<br>NM_011323.2 | 115 | 6191..6305<br>6130..6244 | *CGTGACACGGTTGCATCCT*<br>*ACCGAGTGTGGAACATGCAGTA* |
| Nav1.7 | NM_018852.2 | 106 | 4360..4465 | *CCTTGGCCCCATTAAATCTCT*<br>*TGCTCCTATGAGTGCGTTGAC* |
| Nav1.8 | NM_009134.2 | 81 | 1342..1422 | *TTGACACAACCTCGCTCTATTCC*<br>*ATTTCACCCTGGGTCTTCTCTCA* |
| Nav1.9 | NM_011887 | 81 | 4372..4481 | *CTTCAGGATTGTCCGCTTGG*<br>*AGAGAGAGGGGAGAGACATCATCA* |
| β1 | NM_011322 | 67 | 583..649 | *CACTCTGGCGACTACGAATGTC*<br>*TGGTGTTGTGCTCATAATTATCAA* |
| β2 | NM_001014761 | 132 | 299..430 | *ACCTTCAACTCCTGCTACACCG*<br>*CCGCTCCAGCTTCAGGTTAAT* |
| β3 | NM_153522.2<br>NM_178227.4<br>NM_001083917.1 | 61 | 1169..1229<br>804..864<br>804..864 | *ACCGGCCCTTTGTGAAGAC*<br>*TCTCCCGCCTCTTCAGTGACT* |
| β4 | NM_001013390.2 | 82 | 486..594 | *GACTCTCATCATCCTGGCTGTG*<br>*CTTCTTCTCTCGGGTCTTCTTCAG* |
| HPRT | NM_013556 | 89 | 223..312 | *ATCATTATGCCGAGGATTTGGA*<br>*CCTTCATGACATCTCGAGCAAGT* |
| Arbp | NM_007475.5 | 234 | 829..1062 | *GGTGCCACACTCCATCATCA*<br>*CCGAATCCCATATCCTCATC* |

Prod (bp): amplicon size in base pairs; Pos: amplicon start and finish positions in NCBI Reference Sequence; Seq: targeted sequence, listed first is the forward primer (f), second is the reverse primer (r).

**Table 2.** Primer efficiencies

| Gene | Wildtype | | Nf1+/− | |
|---|---|---|---|---|
| | Slope | Efficiency | Slope | Efficiency |
| Nav1.1 | −3.45±0.05 | 1.949±0.017 | −3.43±0.04 | *1.959±0.015* |
| Nav1.2 | −3.49±0.04 | 1.934±0.015 | −3.43±0.06 | *1.961±0.02.3* |
| Nav1.3 | −3.45±0.17 | 1.965±0.057 | −3.37±0.05 | *1.984±0.021* |
| Nav1.5 | −3.49±0.10 | 1.941±0.037 | −3.33±0.12 | *2.001±0.052* |
| Nav1.6 | −3.59±0.04 | 1.900±0.012 | −3.56±0.04 | *1.911±0.012* |
| Nav1.7 | −3.52±0.02 | 1.925±0.007 | −3.50±0.03 | *1.931±0.012* |
| Nav1.8 | −3.57±0.02 | 1.905±0.006 | −3.55±0.02 | *1.913±0.009* |
| Nav1.9 | −3.44±0.03 | 1.953±0.012 | −3.44±0.03 | *1.954±0.011* |
| β1 | −3.45±0.01 | 1.948±0.003 | −3.46±0.01 | *1.945±0.003* |
| β2 | −3.44±0.05 | 1.956±0.021 | −3.51±0.03 | *1.939±0.008* |
| β3 | −3.37±0.05 | 1.983±0.023 | −3.39±0.04 | *1.974±0.017* |
| β4 | −3.50±0.03 | 1.930±0.010 | −3.43±0.06 | *1.957±0.021* |
| HPRT | −3.62±0.01 | 1.888±0.004 | −3.62±0.01 | *1.888±0.004* |
| *Arbp* | *−3.46±0.02* | *1.947±0.008* | *−3.47±0.02* | *1.942±0.009* |

Values of Nav1.1–1.8, HPRT, Arbp represent means±SEM $n$=7 and 6 for wildtype and *Nf1+/−*, respectively; for Nav1.9 $n$=5 of each genotype and for β1–β4 $n$=4 of each genotype.

skeletal muscle (Trimmer et al., 1989) and Nav1.5 in the heart (Rogart et al., 1989). qPCR reactions were run in triplicate

on an Applied Biosystems 7500 Fast Real-Time PCR System using MicroAmp® Fast 96-well reaction plates sealed with MicroAmp® optical adhesive film. All reactions began with an initial cycle of 95° C for 10 min followed by 40 cycles of 95° C for 15 s and 60° C for 1 min. Whenever possible , efficiencies for each primer pair were determined from the fitted slope of three- to five-point standard curve over a four-log dilution as described in Pfaffl (2001). The regression fit was considered to be acceptable when the $r^2$>0.985, with most values well exceeding 0.990. Calculated efficiencies for all primers are listed in Table 2. The specificity of these amplifications was verified by melt curve analysis with detection of a single peak only and electrophoresis on a 2% agarose gel with detection of only a single band at the appropriate size. In one case, qPCR for Arbp exhibited two peaks for the melt curves and these are believed to result from known splice variants.

*Data analysis*

The quantification cycle (Cq) was chosen to be number of cycles when the value of normalized fluorescence generated by SYBR green emission (ΔRn) attained 0.3. All individual Cq values are the means obtained from triplicate samples. To determine the expression levels of sodium channel mRNA relative to either HPRT or Arbp, a calculation based on Pfaffl (2001) was used. The relative expression ratio of sodium channel subtype to reference gene was defined by:

$$R = (Eff_{NaChan})^{\Delta CqNaChan(WT - Nf1+/-)} / (Eff_{Refgene})^{\Delta CqRefgene(WT - Nf1+/-)}$$

$$Eff_{NaChan} = 10^{-1/slopeNaChan} \qquad Eff_{Refgene} = 10^{-1/slopeRefgene}$$

where $Eff_{NaChan}$ is the average efficiency of the qPCR for each individual sodium channel or β subunit obtained from the wildtype and *Nf1+/-* genotypes; ΔCqNaChan is the difference in average Cq values measured for each individual sodium channel subtype in the wildtype DRG minus that measured in the *Nf1+/-* DRG; $Eff_{Refgene}$ is the average efficiency of the qPCR for either HPRT or Arbp obtained from the wildtype and *Nf1+/-* genotypes; ΔCqRefgene is the difference in the average Cq values measured for either HPRT or Arbp in the wildtype DRG minus that measured in the *Nf1+/-* DRG. The relative expression of the individual sodium channel and β subunit subtypes (*Nf1+/-* compared to wildtype) and the statistical significance of that difference were determined by using the Relative Expression Software Tool wherein the null hypothesis was tested by using a Pair Wise Fixed Reallocation Randomization Test©. The reader is referred to Pfaffl et al. (2002) and REST 2009 (www.gene-quantification.de/rest-2009.html) for a detailed description of this analysis. Values of P<0.05 were considered to be significantly different.

For determination of the distribution of sodium channels and the β subunits in wildtype and *Nf1+/-* mice, the Cq and averaged reaction efficiency were used to estimate the number of copies of each gene as follows, number of $copies_{NaChan} = Eff_{NaChan}^{-Cq}$. The copy numbers for all α subunits were totaled for each animal, this sum then was used to determine the percentage distribution for each α subunit according to the equation % Total = $Copies_{NaChan} / \Sigma Copies_{NaChan\ 1.1\text{-}1.9}$
The mean percentage total was calculated for both wildtype and *Nf1+/-* mice (n=4). The same series of calculations was performed for β subunits using their corresponding Cq and averaged values for reaction efficiencies.

KEY RESEARCH ACCOMPLISHMENTS:

- In wildtype mice, Nav1.9 was the most abundant subtype with Nav1.7 and Nav1.8 the next most abundant
- Nav1.1, Nav1.3, Nav1.7, and Nav1.8 were significantly elevated in DRG isolated from *Nf1+/-* mice
- Nav1.2, Nav1.5, Nav1.6, and Nav1.9 were not significantly altered
- Expression of the auxiliary beta subunits (B1-B4) was not different

REPORTABLE OUTCOMES:

This work was presented as an abstract/poster at the annual meeting of the Children's Tumor foundation (June 2011) and was also be presented at the annual meeting of the Society for Neuroscience (November 2011). **A manuscript entitled "Dorsal root ganglia isolated from *Nf1+/-* mice exhibit increased levels of mRNA expression of voltage-dependent sodium channels" is now in press for publication in the journal *Neuroscience*.** In addition, these outcomes will form the preliminary results for submission of an application to the National Institutes of Health to further investigate the causal mechanisms whereby neurofibromin regulates the expression of sodium changes (e.g. transcriptional factors) and how this relates to changes in pain threshold in NF1 patients. Personal supported by this award were Dr. Grant Nicol, Dr. Cynthia Hingtgen, Dr. Xian Xuan Chi, and Ms. Kathryn Hodgdon.

CONCLUSION:

In the DRG isolated from wildtype mice, the Nav1.9 subtype was the most abundant with Nav1.7 and Nav1.8 being the next most abundant subtypes. For the auxiliary β subunits, β1 was by far the most abundant subtype. The mRNA for the alpha subunits of the sodium channels Nav1.1, Nav1.3, Nav1.7, and Nav1.8 were significantly elevated in DRG isolated from *Nf1+/-* mice. There were no significant changes in the relative expression levels of the auxiliary beta subunits. These results suggest that increased expression levels of Nav1.7, Nav1.8, and perhaps Nav1.1 in the *Nf1+/-* DRG make the largest contribution to the increased sodium current density and thus give rise to the enhanced excitability. Though the mechanisms by which many people with NF1 experience increased pain have not been elucidated, these abnormal painful states may involve elevated expression of specific sodium channel subtypes in small diameter nociceptive sensory neurons.

So what- Until we understand the basic causal mechanisms such as which particular sodium channel subtype is altered in NF1 patients, therapeutic interventions are not possible. This work begins to provide an understanding which can then be used to develop drugs or interventions directed at these targets whereby the enhanced sensitivity to painful stimuli experienced by some patients with NF1 can be resolved.

REFERENCES:

Amaya F, Decosterd I, Samad TA, Plumpton C, Tate S, Mannion RJ, Costigan M, Woolf CJ (2000) Diversity of expression of the sensory neuron-specific TTX-resistant voltage-gated sodium ion channels SNS and SNS2. Mol Cell Neurosci 15:331-342.

Baker MD, Chandra SY, Ding Y, Waxman SG, Wood JN (2003) GTP-induced tetrodotoxin-resistant Na+ current regulates excitability in mouse and rat small diameter sensory neurones. J Physiol 548:373-382.

Berta T, Poirot O, Pertin M, Ji RR, Kellenberger S Decosterd I (2008) Transcriptional and functional profiles of voltage-gated Na(+) channels in injured and non-injured DRG neurons in the SNI model of neuropathic pain. Mol Cell Neurosci 37:196-208.

Bevan S, Chiu SY, Gray PT, Ritchie JM (1985) The presence of voltage-gated sodium, potassium and chloride channels in rat cultured astrocytes. Proc R Soc Lond B Biol Sci 225:299-313.

Black JA, Dib-Hajj S, McNabola K, Jeste S, Rizzo MA, Kocsis JD, Waxman SG (1996) Spinal sensory neurons express multiple sodium channel alpha-subunit mRNAs. Brain Res Mol Brain Res 43:117-131.

Black JA, Liu S, Waxman SG (2009) Sodium channel activity modulates multiple functions in microglia. Glia 57:1072-1081.

Black JA, Newcombe J, Waxman SG (2010) Astrocytes within multiple sclerosis lesions upregulate sodium channel Nav1.5. Brain 133:835-846.

Black JA, Renganathan M, Waxman SG (2002) Sodium channel Na(v)1.6 is expressed along nonmyelinated axons and it contributes to conduction. Brain Res Mol Brain Res 105:19-28.

Blair NT, Bean BP (2002) Roles of tetrodotoxin (TTX)-sensitive Na+ current, TTX-resistant Na+ current, and Ca2+ current in the action potentials of nociceptive sensory neurons. J Neurosci 22:10277-10290.

Catterall WA, Goldin AL, Waxman SG (2005) International Union of Pharmacology. XLVII. Nomenclature and structure-function relationships of voltage-gated sodium channels. Pharmacol Rev 57:397-409.

Creange A, Zeller J, Rostaing-Rigattieri S, Brugieres P, Degos JD, Revuz J, Wolkenstein P (1999) Neurological complications of neurofibromatosis type 1 in adulthood. Brain 122:473-481.

Cregg R, Momin A, Rugiero F, Wood JN, Zhao J (2010) Pain channelopathies. J Physiol 588:1897-1904.

Cummins TR, Aglieco F, Renganathan M, Herzog RI, Dib-Hajj SD, Waxman SG (2001) Nav1.3 sodium channels: rapid repriming and slow closed-state inactivation display quantitative differences after expression in a mammalian cell line and in spinal sensory neurons. J Neurosci 21:5952-5961.

Cummins TR, Dib-Hajj SD, Black JA, Akopian AN, Wood JN, Waxman SG (1999) A novel persistent tetrodotoxin-resistant sodium current in SNS-null and wild-type small primary sensory neurons. J Neurosci 19:RC43.

Cummins TR, Howe JR, Waxman SG (1998) Slow closed-state inactivation: a novel mechanism underlying ramp currents in cells expressing the hNE/PN1 sodium channel. J Neurosci 18:9607-9619.

Cummins TR, Sheets PL, Waxman SG (2007) The roles of sodium channels in nociception: Implications for mechanisms of pain. Pain 131:243-257.

Cummins TR, Waxman SG (1997) Downregulation of tetrodotoxin-resistant sodium currents and upregulation of a rapidly repriming tetrodotoxin-sensitive sodium current in small spinal sensory neurons after nerve injury. J Neurosci 17:3503-3514.

Daston MM, Scrable H, Nordlund M, Sturbaum AK, Nissen LM, Ratner N (1992) The protein product of the neurofibromatosis type 1 gene is expressed at highest abundance in neurons, Schwann cells, and oligodendrocytes. Neuron 8:415-428.
Dib-Hajj S, Black JA, Felts P, Waxman SG (1996) Down-regulation of transcripts for Na channel alpha-SNS in spinal sensory neurons following axotomy. Proc Natl Acad Sci USA 93:14950-14954.
Dib-Hajj SD, Cummins TR, Black JA, Waxman SG (2010) Sodium channels in normal and pathological pain. Annu Rev Neurosci 33:325-347.
Docherty RJ, Farmer CE (2009) The pharmacology of voltage-gated sodium channels in sensory neurones. Handb Exp Pharmacol 194:519-561.
Duan JH, Wang Y, Duarte D, Vasko MR, Nicol GD, Hingtgen CM (2011) Ras signaling pathways mediate NGF-induced enhancement of excitability of small-diameter capsaicin-sensitive sensory neurons from wildtype but not *Nf1+/-* mice. Neurosci Lett 496:70-74.
Felts PA, Yokoyama S, Dib-Hajj S, Black JA, Waxman SG (1997)Sodium channel alpha-subunit mRNAs I, II, III, NaG, Na6 and hNE (PN1): different expression patterns in developing rat nervous system. Brain Res Mol Brain Res 45:71-82.
Friedman JM (1999) Epidemiology of neurofibromatosis type 1. Am J Med Genet 89:1-6.
Fukuoka T, Kobayashi K, Yamanaka H, Obata K, Dai Y, Noguchi K (2008) Comparative study of the distribution of the alpha-subunits of voltage-gated sodium channels in normal and axotomized rat dorsal root ganglion neurons. J Comp Neurol 510:188-206.
Goldin AL (2001) Resurgence of sodium channel research. Annu Rev Physiol 63:871-94.
Harper AA, Lawson SN (1985a) Conduction velocity is related to morphological cell type in rat dorsal root ganglion neurones. J Physiol 359:31-46.
Harper AA, Lawson SN (1985b) Electrical properties of rat dorsal root ganglion neurones with different peripheral nerve conduction velocities. J Physiol 359:47-63.
Hemmick LM, Perney TM, Flamm RE, Kaczmarek LK, Birnberg NC (1992) Expression of the H-ras oncogene induces potassium conductance and neuron-specific potassium channel mRNAs in the AtT20 cell line. J Neurosci 12:2007-2014.
Herzog RI, Cummins TR, Waxman SG (2001) Persistent TTX-resistant Na+ current affects resting potential and response to depolarization in simulated spinal sensory neurons. J Neurophysiol 86:1351-1364.
Ho C, O'Leary ME (2011) Single-cell analysis of sodium channel expression in dorsal root ganglion neurons. Mol Cell Neurosci 46:159-166.
Isom LL (2001) Sodium channel beta subunits: anything but auxiliary. Neuroscientist 7:42-54.
Jacks T, Shih TS, Schmitt EM, Bronson RT, Bernards A, Weinberg RA (1994) Tumour predisposition in mice heterozygous for a targeted mutation in Nf1. Nat Genet 7:353-361.
Jarecki BW, Piekarz AD, Jackson JO 2nd, Cummins TR (2010) Human voltage-gated sodium channel mutations that cause inherited neuronal and muscle channelopathies increase resurgent sodium currents. J Clin Invest 120:369-378.
Jarecki BW, Sheets PL, Jackson JO 2nd, Cummins TR (2008) Paroxysmal extreme pain disorder mutations within the D3/S4-S5 linker of Nav1.7 cause moderate destabilization of fast inactivation. J Physiol 586:4137-4153.
Largaespada DA, Brannan CI, Jenkins NA, Copeland NG (1996) Nf1 deficiency causes Ras-mediated granulocyte/macrophage colony stimulating factor hypersensitivity and chronic myeloid leukaemia. Nat Genet 12:137-143.
Lau NB, Feldkamp MM, Roncari L, Loehr AH, Shannon P, Gutmann DH, Guha, A (2000) Loss of neurofibromin is associated with activation of RAS/MAPK and PI3-K/AKT signaling in a Neurofibromatosis 1 astrocytoma. J Neuropathol Exp Neurol 59:759-767.
Lawson SN (2002) Phenotype & function of somatic primary afferent nociceptive neurones with C-, Aδ or Aα/β-fibres. J Exp Physiol 87:239–244.
Patino GA, Isom LL (2010) Electrophysiology and beyond: multiple roles of Na+ channel β subunits in development and disease. Neurosci Lett 486:53-59.
Pfaffl MW (2001) A new mathematical model for relative quantification in real-time RT-PCR. Nucleic Acids Res 29:e45.
Pfaffl MW, Horgan GW, Dempfle L (2002) Relative expression software tool (REST) for group-wise comparison and statistical analysis of relative expression results in real-time PCR. Nucleic Acids Res 30:e36.
Rane SG (1991) A Ca2(+)-activated K+ current in ras-transformed fibroblasts is absent from nontransformed cells. Am J Physiol 260:C104-C112.
Renganathan M, Cummins TR, Waxman SG (2001) Contribution of Na(v)1.8 sodium channels to action potential electrogenesis in DRG neurons. J Neurophysiol 86:629-640.

Rogart RB, Cribbs LL, Muglia LK, Kephart DD, Kaiser MW (1989) Molecular cloning of a putative tetrodotoxin-resistant rat heart Na+ channel isoform. Proc Natl Acad Sci USA 86:8170-8174.
Rush AM, Cummins TR, Waxman SG (2007) Multiple sodium channels and their roles in electrogenesis within dorsal root ganglion neurons. J Physiol 579:1-14.
Trimmer JS, Cooperman SS, Tomiko SA, Zhou JY, Crean SM, Boyle MB, Kallen RG, Sheng ZH, Barchi RL, Sigworth FJ, et al. (1989) Primary structure and functional expression of a mammalian skeletal muscle sodium channel. Neuron 3:33-49.
Wang JG, Strong JA, Xie W, Yang RH, Coyle DE, Wick DM, Dorsey ED, Zhang JM (2008) The chemokine CXCL1/growth related oncogene increases sodium currents and neuronal excitability in small diameter sensory neurons. Mol Pain 4:38.
Wang Y, Duan JH, Hingtgen CM, Nicol GD (2010) Augmented sodium currents contribute to the enhanced excitability of small diameter capsaicin-sensitive sensory neurons isolated from Nf1+/- mice. J Neurophysiol 103:2085-2094.
Wang Y, Nicol GD, Clapp DW, Hingtgen CM (2005) Sensory neurons from Nf1 haploinsufficient mice exhibit increased excitability. J Neurophysiol 94: 3670-3676.
Waxman SG, Kocsis JD, Black JA (1994) Type III sodium channel mRNA is expressed in embryonic but not adult spinal sensory neurons, and is reexpressed following axotomy. J Neurophysiol 72:466-470.
Waxman SG, Sontheimer H, Black JA, Minturn JE, Ransom BR (1993) Dynamic aspects of sodium channel expression in astrocytes. Adv Neurol 59:135-155.
Wolkenstein P, Zeller J, Revuz J, Ecosse E, Leplege A (2001) Quality-of-life impairment in neurofibromatosis type 1: a cross-sectional study of 128 cases. Arch Dermatol 137:1421-1425.
Vogel KS, Brannan CI, Jenkins NA, Copeland NG, Parada LF (1995) Loss of neurofibromin results in neurotrophin-independent survival of embryonic sensory and sympathetic neurons. Cell 82:733-742.
Zhang YY, Vik TA, Ryder JW, Srour EF, Jacks T, Shannon K, Clapp DW (1998) Nf1 regulates hematopoietic progenitor cell growth and ras signaling in response to multiple cytokines. J Exp Med 187:1893-1902.

APPENDICES: One appendix file (Hodgden correct proof.pdf) is included. It is the corrected proof of our publication that will appear in Neuroscience sometime in 2012.

Please cite this article in press as: Hodgdon KE, et al., Dorsal root ganglia isolated from *Nf1*+/− mice exhibit increased levels of mRNA expression of . . . , Neuroscience (2012), doi: 10.1016/j.neuroscience.2011.12.045

*Neuroscience* xx (2012) xxx

# DORSAL ROOT GANGLIA ISOLATED FROM *Nf1*+/− MICE EXHIBIT INCREASED LEVELS OF mRNA EXPRESSION OF VOLTAGE-DEPENDENT SODIUM CHANNELS

**K. E. HODGDON,[a] C. M. HINGTGEN[a,b] AND G. D. NICOL[a]***

[a]*Department of Pharmacology and Toxicology, Indiana University School of Medicine, Indianapolis, IN 46202, USA*

[b]*Department of Neurology, School of Medicine, Indiana University, Indianapolis, IN 46202, USA*

**Abstract—We reported previously that sensory neurons isolated from mice with a heterozygous mutation of the *Nf1* gene (*Nf1*+/−) exhibited greater excitability and increased sodium current densities compared with wildtype mice. This raises the question as to whether the increased current density resulted from post-translational modifications or increased expression of sodium channels. Quantitative real-time polymerase chain reaction was used to measure expression levels of the nine different voltage-gated sodium channel $\alpha$ subunits and the four associated auxiliary $\beta$ subunits in the dorsal root ganglia (DRG) obtained from wildtype and *Nf1*+/− mice. The Relative Expression Software Tool indicated that Nav1.1, Nav1.3, Nav1.7, and Nav1.8 were significantly elevated in DRG isolated from *Nf1*+/− mice. Expression of Nav1.2, Nav1.5, Nav1.6, and Nav1.9 were not significantly altered. The gene transcript for Nav1.4 was not detected. There were no significant changes in the relative expression levels of $\beta$ subunits. The Nav1.9 subtype was the most abundant with Nav1.7 and Nav1.8 being the next most abundant subtypes, whereas Nav1.3 was relatively less abundant. For the $\beta$ subunits, $\beta$1 was by far the most abundant subtype. These results demonstrate that the increased expression levels of Nav1.7, Nav1.8, and perhaps Nav1.1 in the *Nf1*+/− DRG make the largest contribution to the increased sodium current density and thus give rise to the enhanced excitability. Though the mechanisms by which many people with NF1 experience increased pain have not been elucidated, these abnormal painful states may involve elevated expression of specific sodium channel subtypes in small diameter nociceptive sensory neurons. © 2012 Published by Elsevier Ltd on behalf of IBRO.**

**Key words: neurofibromin, qPCR, sensory neuron.**

Neurofibromatosis type 1 (NF1) is an autosomal dominant disorder with an incidence of 1 in 3000 people and is characterized by numerous abnormalities that include benign neurofibromas, malignant peripheral tumors of the nerve sheath, astrocytomas, bone deformities, and myeloid leukemias (Friedman, 1999). Some people with NF1 experience greater intensities of painful sensations to different stimuli, such as minor injuries, than those without this genetic disorder (Créange et al., 1999; Wolkenstein et al., 2001). NF1 is a consequence of a heterozygous mutation of the *NF1* gene (*NF1*+/−), which results in reduced expression of functional neurofibromin, the product of the *NF1* gene. Neurofibromin is richly expressed in the nervous system (Daston et al., 1992) and promotes hydrolysis of Ras (Ras-GTP) to its inactive form (Ras-GDP) by serving as a GTPase activating protein (GAP). Mutations of *NF1* or the mouse ortholog *Nf1* frequently result in enhanced basal and cytokine-stimulated Ras activity in many cell types, including sensory neurons (Largaespada et al., 1996; Vogel et al., 1995; Zhang et al., 1998; Lau et al., 2000). Increased Ras activity may influence protein expression levels. For example, expression of a GAP-resistant Ras in AtT20 cells induced expression of a potassium channel that greatly shortened the duration of the action potential and led to repetitive action potential firing (Hemmick et al., 1992). Similarly, Ras transformation of a fibroblast cell line lead to the expression of a $Ca^{2+}$-dependent potassium current that was not detected in non-transformed cells (Rane, 1991). These studies suggest that the heterozygous deletion of neurofibromin and altered Ras signaling can play a critical role in regulating the expression of ion channels that set the level of neuronal excitability.

We reported previously that small diameter, capsaicin-sensitive sensory neurons isolated from *Nf1*+/− mice exhibited augmented excitability (Wang et al., 2005) and that this enhanced excitability was likely the result of increased sodium current densities (Wang et al., 2010). Voltage-dependent sodium currents are critical in producing the upstroke of the action potential, which is the key component of neural communication. Molecularly, the $\alpha$ subunits of mammalian sodium channels have been categorized into one family consisting of nine different subtypes (Nav1.1–Nav1.9) (Goldin, 2001; Catterall et al., 2005). Pharmacologically, sodium channels have been classified according to their sensitivity to the blocker tetrodotoxin (TTX) wherein the currents conducted by Nav1.1–1.4, 1.6, and 1.7 are completely blocked, whereas the currents carried by Nav1.5, Nav1.8, and Nav1.9 are resistant or insensitive to inhibition by the toxin. The TTX-sensitive sodium currents exhibit both rapid activation and inactivation properties, whereas the TTX-resistant subtypes activate and inactivate more slowly. The properties of these different subtypes of sodium channels have been reviewed recently (Goldin, 2001; Catterall et al., 2005; Dib-Hajj et al., 2010). Associated with the $\alpha$ subunits are the modulatory $\beta$ subunits of which four different subtypes exist ($\beta$1–$\beta$4). The $\beta$ subunits modulate

*Corresponding author. Tel: +1-317-274-1570; fax: +1-317-274-7714.
E-mail address: gnicol@iupui.edu (G. D. Nicol).

*Abbreviations:* Arbp, acidic ribosomal protein P0; Cq, quantification cycle; DRG, dorsal root ganglion; HPRT, hypoxanthine-guanine phosphoribosyl transferase; PCR, polymerase chain reaction; qPCR, quantitative PCR; NF1, Neurofibromatosis type 1; TTX, tetrodotoxin.

0306-4522/12 $36.00 © 2012 Published by Elsevier Ltd on behalf of IBRO.
doi:10.1016/j.neuroscience.2011.12.045

the amplitude and kinetics of the currents conducted by the $\alpha$ subunits and also influence the trafficking and expression of the $\alpha$ subunits (reviewed by Isom, 2001; Patino and Isom, 2010). To determine the possible mechanisms giving rise to the augmented neuronal firing and sodium current density in *Nf1*+/− sensory neurons, the relative expression levels of mRNA for the $\alpha$ subtypes and $\beta$ subunits of voltage-gated sodium channels were determined in wildtype and *Nf1*+/− neurons of the dorsal root ganglion (DRG). Consistent with our physiological observations, DRG obtained from *Nf1*+/− mice exhibited increased levels for some but not all $\alpha$ subunits, whereas the $\beta$ subunits were not altered.

## EXPERIMENTAL PROCEDURES

### Animals

Mice heterozygous for the *Nf1* mutation on a background of C57BL/6J were originally developed by Dr. Tyler Jacks (Jacks et al., 1994). All animals were housed, bred, and had free access to food and water in the Indiana University Laboratory Animal Research Center and were used in accordance with National Institute of Health Guide for Care and Use of Laboratory Animals (National Institutes of Health Publications No. 80–23, revised 1996). These procedures were designed to minimize the number and suffering of the animals. All procedures were approved by the Animal Use and Care Committee of the Indiana University School of Medicine.

### Isolation of the dorsal root ganglia

The DRG were isolated from young adult C57BL6J mice (2–3 months old). The wildtype and *Nf1*+/− mice used in these studies were littermates. Briefly, mice were killed by placing them in a $CO_2$ chamber, and the spinal column was removed. Lumbar, cervical, and thoracic DRG were collected and trimmed in cold, sterilized Puck's solution composed of (in mM): 171 NaCl, 6.7 KCl, 1.6 $Na_2PO_4$, 0.5 $KH_2PO_4$, 6 d-glucose, and 0.01% phenol red, pH 7.3. The ganglia were then transferred to a conical tube and washed with sterilized PBS. Tissues were stored at −80 °C and used within two weeks.

### Real-time quantitative PCR (qPCR)

Total RNA was extracted from DRG tissue using the RNeasy® Plus Minikit (Qiagen, Valencia, CA, USA) and assessed on a NanoDrop ND-1000 Spectrophotometer (Thermoscientific, Franklin, MA, USA) for concentration ($A_{260}$) and purity by OD ratios ($A_{260}/A_{280}$, ranging between 2.0 and 2.2). Following treatment with DNase I (Invitrogen, Carlsbad, CA, USA) to eliminate any residual genomic DNA, 1 $\mu$g RNA was reversed transcribed using the iScript cDNA Synthesis Kit (Bio-Rad, Hercules, CA, USA) in 20 $\mu$l reactions according to the manufacturer's instructions. To assess the specificity of these reactions, no reverse transcriptase (RT) and no template controls also were generated. cDNA was stored at −20 °C before polymerase chain reaction (PCR) detection. Reverse transcription products were diluted and amplified in 25 $\mu$l reactions using Power SYBR® Green PCR Master Mix (Applied Biosystems, Carlsbad, CA, USA) and 500 nM forward and reverse primers (Invitrogen). Sodium channel primers were designed specifically against mouse transcripts using PrimerExpress® software v3.0 (Applied Biosystems) and were based on a previous publication (Wang et al., 2008) describing PCR amplification of mRNA for voltage-dependent sodium channels in rat DRG. Hypoxanthine-guanine phosphoribosyl transferase (HPRT) and acidic ribosomal protein P0 (Arbp) were selected as reference genes for normalization of the qPCR results. The accession number(s), amplicon size and position, and primer sequences for all genes targeted in this study are shown in Table 1. Primers were initially tested in tissues known to express the targeted sodium channel subtype, for example, Nav1.4 was detected in skeletal muscle (Trimmer et al., 1989) and Nav1.5 in the heart (Rogart et al., 1989). qPCR reactions were run in triplicate on an Applied Biosystems 7500 Fast Real-time PCR System using MicroAmp® Fast 96-well reaction plates sealed with MicroAmp® optical adhesive film. All reactions began with an initial cycle of 95 °C for 10 min followed by 40 cycles of 95 °C for 15 s and 60 °C for 1 min. Whenever possible, efficiencies for each primer pair were determined from the fitted slope of three- to five-point standard curve over a four-log dilution as described in Pfaffl (2001). The regression fit was considered to be acceptable when the $r^2 > 0.985$, with most values well exceeding 0.990. Calculated efficiencies for all primers are listed in Table 2. The specificity of these amplifications was verified by melt curve analysis with detection of a single peak only and electrophoresis on a 2% agarose gel with detection of only a single band at the appropriate size. In one case, qPCR for Arbp exhibited two peaks for the melt curves, and these are believed to result from known splice variants.

### Data analysis

The quantification cycle (Cq) was chosen to be number of cycles when the value of normalized fluorescence generated by SYBR Green emission ($\Delta$Rn) attained 0.3. All individual Cq values are the means obtained from triplicate samples. To determine the expression levels of sodium channel mRNA relative to either HPRT or Arbp, a calculation based on Pfaffl (2001) was used. The relative expression ratio of sodium channel subtype to reference gene was defined by:

$$R = (Eff_{NaChan})^{\Delta CqNaChan(WT-Nf1+/-)} / (Eff_{Refgene})^{\Delta CqRefgene(WT-Nf1+/-)}$$

$$Eff_{NaChan} = 10^{-1/slopeNaChan},\ Eff_{Refgene} = 10^{-1/slopeRefgene}$$

where $Eff_{NaChan}$ is the average efficiency of the qPCR for each individual sodium channel or $\beta$ subunit obtained from the wildtype and *Nf1*+/− genotypes; $\Delta$CqNaChan is the difference in average Cq values measured for each individual sodium channel subtype in the wildtype DRG minus that measured in the *Nf1*+/−DRG; $Eff_{Refgene}$ is the average efficiency of the qPCR for either HPRT or Arbp obtained from the wildtype and *Nf1*+/− genotypes; $\Delta$CqRefgene is the difference in the average Cq values measured for either HPRT or Arbp in the wildtype DRG minus that measured in the *Nf1*+/−DRG. The relative expression of the individual sodium channel and $\beta$ subunit subtypes (*Nf1*+/− compared with wildtype) and the statistical significance of that difference were determined by using the Relative Expression Software Tool (REST) wherein the null hypothesis was tested by using a Pair Wise Fixed Reallocation Randomization Test©. The reader is referred to Pfaffl et al. (2002) and REST 2009 (http://www.gene-quantification.de/rest-2009.html) for a detailed description of this analysis. Values of $P<0.05$ were considered to be significantly different.

For determination of the distribution of sodium channels and the $\beta$ subunits in wildtype and *Nf1*+/− mice, the Cq and averaged reaction efficiency were used to estimate the number of copies of each gene as follows, number of $copies_{NaChan} = Eff_{NaChan}^{-Cq}$. The copy numbers for all $\alpha$ subunits were totaled for each animal, this sum then was used to determine the percentage distribution for each $\alpha$ subunit according to the equation % total$= Copies_{NaChan} / \Sigma\ Copies_{NaChan\ 1.1–1.9}$.

The mean percentage total was calculated for both wildtype and *Nf1*+/− mice ($n=4$). The same series of calculations was performed for $\beta$ subunits using their corresponding Cq and averaged values for reaction efficiencies.

## RESULTS

Our previous studies indicated that sensory neurons isolated from *Nf1*+/− mice exhibited increased excitability

Please cite this article in press as: Hodgdon KE, et al., Dorsal root ganglia isolated from *Nf1*+/− mice exhibit increased levels of mRNA expression of . . . , Neuroscience (2012), doi: 10.1016/j.neuroscience.2011.12.045

**Table 1.** Primer sequences

| Gene | Accession no. | Prod (bp) | Pos | *Seq (5′–3′)* |
|---|---|---|---|---|
| Nav1.1 | NM_018733.2 | 123 | 4465..4587 | *f-CATGTATGCTGCAGTTGATTCCA* |
| | | | | *r-AACAGGTTCAGGGTAAAGAAGG* |
| Nav1.2 | NM_001099298.2 | 82 | 2992..3073 | *GCCTTGCTCCTCAGTTCTTTCA* |
| | | | | *CGGCTATCTGGAGGTTGTTCA* |
| Nav1.3 | NM_018732.3 | 95 | 4153..4247 | *GGTGTGCCTCATCTTCTGGTTAA* |
| | | | | *TGCTGCCCGTTGTCATGTTA* |
| Nav1.4 | NM_133199.2 | 94 | 391..484 | *CGCGCTGTTCAGCATGTT* |
| | | | | *CTCCACGTCCTTGGACCAAG* |
| Nav1.5 | NM_021544.3 | 83 | 1142..1224 | *ACCTCAATGACCCAGCCAATTA* |
| | | | | *TGTCCCGGCATCAGAGCT* |
| Nav1.6 | NM_001077499.1 | 115 | 6191..6305 | *CGTGACACGGTTGCATCCT* |
| | NM_011323.2 | | 6130..6244 | *ACCGAGTGTGGAACATGCAGTA* |
| Nav1.7 | NM_018852.2 | 106 | 4360..4465 | *CCTTGGCCCCATTAAATCTCT* |
| | | | | *TGCTCCTATGAGTGCGTTGAC* |
| Nav1.8 | NM_009134.2 | 81 | 1342..1422 | *TTGACACAACCTCGCTCTATTCC* |
| | | | | *ATTTCACCCTGGGTCTTCTCTCA* |
| Nav1.9 | NM_011887 | 81 | 4372..4481 | *CTTCAGGATTGTCCGCTTGG* |
| | | | | *AGAGAGAGGGGAGAGACATCATCA* |
| $\beta$1 | NM_011322 | 67 | 583..649 | *CACTCTGGCGACTACGAATGTC* |
| | | | | *TGGTGTTGTGCTCATAATTATCAA* |
| $\beta$2 | NM_001014761 | 132 | 299..430 | *ACCTTCAACTCCTGCTACACCG* |
| | | | | *CCGCTCCAGCTTCAGGTTAAT* |
| $\beta$3 | NM_153522.2 | 61 | 1169..1229 | *ACCGGCCCTTTGTGAAGAC* |
| | NM_178227.4 | | 804..864 | *TCTCCCGCCTCTTCAGTGACT* |
| | NM_001083917.1 | | 804..864 | |
| $\beta$4 | NM_001013390.2 | 82 | 486..594 | *GACTCTCATCATCCTGGCTGTG* |
| | | | | *CTTCTTCTCTCGGGTCTTCTTCAG* |
| HPRT | NM_013556 | 89 | 223..312 | *ATCATTATGCCGAGGATTTGGA* |
| | | | | *CCTTCATGACATCTCGAGCAAGT* |
| Arbp | NM_007475.5 | 234 | 829..1062 | *GGTGCCACACTCCATCATCA* |
| | | | | *CCGAATCCCATATCCTCATC* |

Prod (bp): amplicon size in base pairs; Pos: amplicon start and finish positions in NCBI Reference Sequence; Seq: targeted sequence, listed first is the forward primer (f), second is the reverse primer (r).

that resulted from elevated levels of voltage-dependent sodium currents (Wang et al., 2005, 2010). To determine if the augmented sodium currents were a consequence of increased expression of sodium channel mRNA, quantitative PCR was performed using DRG isolated from wildtype and *Nf1*+/− mice. The average Cq values obtained for

**Table 2.** Primer efficiencies

| Gene | Wildtype | | Nf1+/− | |
|---|---|---|---|---|
| | Slope | Efficiency | Slope | Efficiency |
| Nav1.1 | −3.45±0.05 | 1.949±0.017 | −3.43±0.04 | *1.959±0.015* |
| Nav1.2 | −3.49±0.04 | 1.934±0.015 | −3.43±0.06 | *1.961±0.02.3* |
| Nav1.3 | −3.45±0.17 | 1.965±0.057 | −3.37±0.05 | *1.984±0.021* |
| Nav1.5 | −3.49±0.10 | 1.941±0.037 | −3.33±0.12 | *2.001±0.052* |
| Nav1.6 | −3.59±0.04 | 1.900±0.012 | −3.56±0.04 | *1.911±0.012* |
| Nav1.7 | −3.52±0.02 | 1.925±0.007 | −3.50±0.03 | *1.931±0.012* |
| Nav1.8 | −3.57±0.02 | 1.905±0.006 | −3.55±0.02 | *1.913±0.009* |
| Nav1.9 | −3.44±0.03 | 1.953±0.012 | −3.44±0.03 | *1.954±0.011* |
| $\beta$1 | −3.45±0.01 | 1.948±0.003 | −3.46±0.01 | *1.945±0.003* |
| $\beta$2 | −3.44±0.05 | 1.956±0.021 | −3.51±0.03 | *1.939±0.008* |
| $\beta$3 | −3.37±0.05 | 1.983±0.023 | −3.39±0.04 | *1.974±0.017* |
| $\beta$4 | −3.50±0.03 | 1.930±0.010 | −3.43±0.06 | *1.957±0.021* |
| HPRT | −3.62±0.01 | 1.888±0.004 | −3.62±0.01 | *1.888±0.004* |
| *Arbp* | *−3.46±0.02* | *1.947±0.008* | *−3.47±0.02* | *1.942±0.009* |

Values of Nav1.1–1.8, HPRT, Arbp represent means±SEM $n$=7 and 6 for wildtype and *Nf1*+/−, respectively; for Nav1.9 $n$=5 of each genotype and for $\beta$1–$\beta$4 $n$=4 of each genotype.

Please cite this article in press as: Hodgdon KE, et al., Dorsal root ganglia isolated from *Nf1*+/− mice exhibit increased levels of mRNA expression of . . . , Neuroscience (2012), doi: 10.1016/j.neuroscience.2011.12.045

**Table 3.** Cq values

| Gene | Wildtype | Nf1+/− |
|---|---|---|
| Nav1.1 | 27.44±0.48 | *26.95±0.10* |
| Nav1.2 | 31.38±0.37 | *31.07±0.13* |
| Nav1.3 | 33.07±0.62 | *32.32±0.09* |
| Nav1.5 | 31.71±0.45 | *31.24±0.20* |
| Nav1.6 | 27.54±0.44 | *27.12±0.26* |
| Nav1.7 | 26.58±0.53 | *25.94±0.14* |
| Nav1.8 | 26.30±0.43 | *25.83±0.19* |
| Nav1.9 | 23.63±0.34 | *23.93±0.15* |
| β1 | 24.37±0.26 | *24.55±0.15* |
| β2 | 28.37±0.34 | *28.24±0.17* |
| β3 | 26.75±0.28 | *26.95±0.08* |
| β4 | 26.48±0.33 | *26.34±0.24* |
| HPRT | 24.79±0.29 | *24.66±0.20* |
| *Arbp* | *21.36±0.12* | *21.31±0.19* |

Values of Nav1.1–1.8, HPRT, Arbp represent means±SEM $n=7$ and 6 for wildtype and *Nf1*+/−, respectively; for Nav1.9 $n=5$ of each genotype and for β1–β4 $n=4$ of each genotype.

eight of the nine different voltage-dependent α subunits and the four auxiliary β subunits are summarized in Table 3. The Cq values indicate that in wildtype mice Nav1.9 (23.63±0.34, $n=5$ mice) was the most abundant channel subtype with Nav1.7 (26.58±0.53, $n=7$ mice) and Nav1.8 (26.30±0.43, $n=7$ mice) being the next most abundant subtypes, whereas Nav1.3 was less abundant (33.07±0.62, $n=7$ mice). For the β subunits, β1 was by far the most abundant subtype and β2 the least abundant. The gene transcripts for Nav1.4 were not detected in the DRG, consistent with previous observations that the expression of Nav1.4 is limited to skeletal muscle (Trimmer et al., 1989). The primers used in our study were capable of detecting Nav1.4 in mRNA isolated from mouse skeletal muscle (Cq=26.25±0.05, data not shown).

To assess whether there were differences in the mRNA levels for these sodium channels between the two genotypes, the expression of sodium channel subtypes was normalized to two reference genes, HPRT and Arbp. The relative differences in channel expression were determined by using a method described by Pfaffl (2001) wherein the Cq values are corrected by accounting for the efficiency of the PCR for both the targeted and reference genes. The relative expression for the α subunits of sodium channel subtypes determined in the *Nf1*+/− mice compared with the wildtype is summarized in Fig. 1A. An analysis using the REST protocol indicated that Nav1.1 (1.67-fold), Nav1.3 (2.04-fold), Nav1.7 (1.87-fold), and Nav1.8 (1.48-fold) were elevated significantly ($P<0.05$) in the DRG isolated from *Nf1*+/− mice compared with the wildtype. The expression of Nav1.2 (1.27-fold), Nav1.5 (1.52-fold), Nav1.6 (1.42-fold), and Nav1.9 (0.65-fold) were not significantly altered. In addition, as summarized in Fig. 1B, there were no significant differences in the relative expression of β subunits. These results demonstrate that the expression of some sodium channel subtypes is increased in *Nf1*+/− mice and therefore could account for the elevated excitability and sodium current densities recorded from *Nf1*+/− neurons.

This observation raises the question as to whether there are changes in the contribution of individual sodium channel subtypes to the total mRNA pool in these genotypes that could account for the elevated sodium current densities in the *Nf1*+/− sensory neurons. The fractional contribution of each channel subtype to the total mRNA copy number is illustrated in Fig. 2. The results were obtained from four mice of each genotype wherein qPCR was performed for Nav1.1–Nav1.9 and β1–β4. The copy number ($Eff^{-Cq}$) for each channel was calculated, and the total value was determined for each mouse. The average copy number for each channel subtype was determined for the four mice of each genotype. The fractional contribution of each channel subtype was then assessed by dividing the average copy number for each channel by the average total. Overall, there was not a significant difference between the genotypes in the fractional contribution of a particular channel subtype to the total sodium channel mRNA (Fig. 2A). However, based on the average values, there is a trend toward higher fractional levels of Nav1.6, Nav1.7, and Nav1.8 in the *Nf1*+/−DRG compared with the wildtype. The largest contributors to the total mRNA were the TTX-resistant sodium channels Nav1.9 (42.9 and 43.1% in the wildtype and *Nf1*+/− neurons, respectively) and Nav1.8 (16.0 and 21.3% in the wildtype and *Nf1*+/− neurons, respectively). Of the TTX-sensitive sodium channels Nav1.6 (8.1 and 10.8% in the wildtype and *Nf1*+/− neurons, respectively) and Nav1.7 (11.2 and 15.3% in the wildtype and *Nf1*+/− neurons, respectively) made the largest contribution. Nav1.2, Nav1.3, and Nav1.5 made only a small contribution

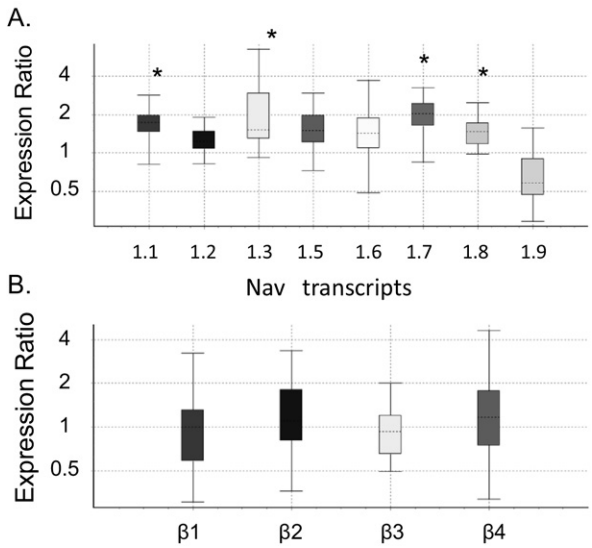


**Fig. 1.** mRNA expression of some sodium channel subtypes is elevated in the DRG of *Nf1*+/− mice compared with wildtype mice. Panel (A) represents the relative expression levels for eight of the nine sodium channel subtypes relative to the reference genes HPRT and Arbp obtained with the REST analysis protocol. The expression of Nav1.1, Nav1.3, Nav1.7, and Nav1.8 were significantly increased ($P<0.05$) in the *Nf1*+/−DRG compared with the wildtype DRG. Panel (B) illustrates the relative expression levels for the auxiliary β subunits relative to HPRT and Arbp. The asterisks indicate a statistical difference ($P<0.05$) using the Relative Expression Software Tool (REST, 2009).

Please cite this article in press as: Hodgdon KE, et al., Dorsal root ganglia isolated from *Nf1*+/− mice exhibit increased levels of mRNA expression of . . . , Neuroscience (2012), doi: 10.1016/j.neuroscience.2011.12.045

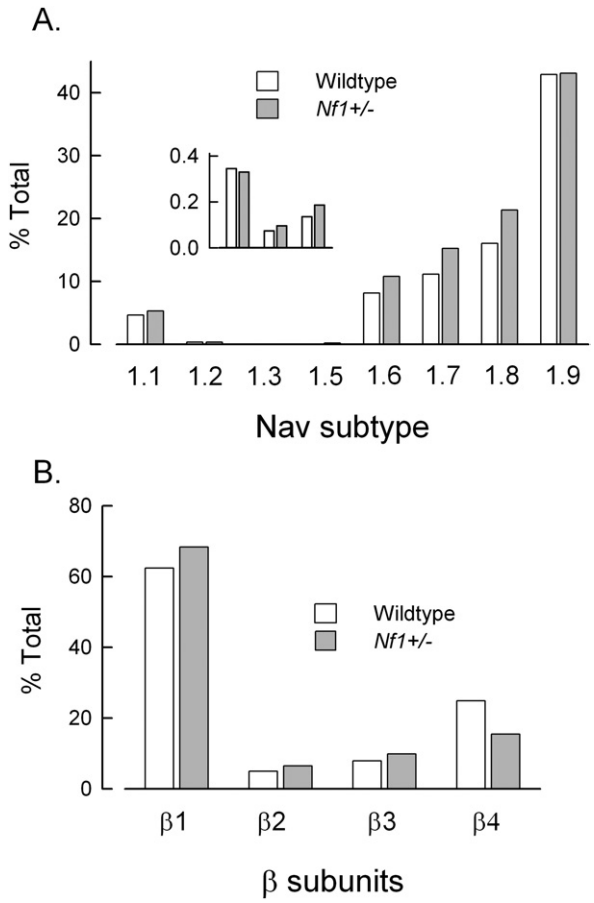


**Fig. 2.** The fractional contributions of individual sodium channel subtypes to the total mRNA are not different between *Nf1*+/− and wildtype DRG. Panel (A) shows that percentage contribution of each $\alpha$ subtype to the total number of sodium channel copies. There appears to be a trend toward higher levels of Nav1.1, Nav1.6, Nav1.7, and Nav1.8 in the Nf1+/−DRG. Panel (B) shows that percentage contribution of each $\beta$ subunit to the total number of $\beta$ copies with a trend toward less $\beta$4 in the *Nf1*+/−DRG.

(<1%) and are shown in the inset of Fig. 2A. Of the $\beta$ subunits, $\beta$1 comprised more than 60% of the total mRNA for these auxiliary subunits in both wildtype and *Nf1*+/− sensory neurons (see Fig. 2B). There is a trend toward a higher fractional contribution of $\beta$1 in the *Nf1*+/−DRG (68.3%) compared with the wildtype DRG (62.3%) and a lower fractional contribution of $\beta$4 in the *Nf1*+/−DRG (15.4%) compared with the wild-type DRG (24.9%). Therefore, these results demonstrate that despite an increase in the overall expression of Nav1.1, Nav1.3, Nav1.7, and Nav1.8, the patterns of predominance remain similar between genotypes. This supports the change in excitability that we have observed previously (Wang et al., 2005, 2010), but suggests that a change in the phenotype of the sensory neuron, for example to a more TTX-sensitive form, does not occur.

## DISCUSSION

The results reported here indicate that expression of the sodium channel subtypes Nav1.1, Nav1.3, Nav1.7, and Nav1.8 were elevated significantly in the DRG isolated from *Nf1*+/− mice compared with wildtype mice. Similar values for the increases in these channel subtypes were observed using either reference gene, HPRT or Arbp, indicating the stability of these genes for the normalization of channel expression. The elevated levels of sodium channel mRNA are consistent with our previous reports that sensory neurons isolated from the DRG of *Nf1*+/− mice generated twofold more action potentials in response to the same level of current stimulation (Wang et al., 2005) and that the sodium current density for both TTX-sensitive and TTX-resistant currents was significantly elevated in the *Nf1*+/− sensory neurons (Wang et al., 2010). Furthermore, expression levels of the $\beta$ subunits were measured as these subunits modulate the amplitude and kinetics of the currents conducted by the $\alpha$ subunits and can also influence the trafficking and surface density of the $\alpha$ subunits (reviewed by Isom, 2001; Patino and Isom, 2010). However, there were no differences in the expression levels of the auxiliary $\beta$ subunits between the two genotypes suggesting that altered $\beta$ subunit expression does not contribute to the increased sodium current densities in *Nf1*+/− sensory neurons.

The neurons of the DRG are a heterogeneous population and are activated by a variety of sensory modalities. The reader is referred to the following reviews regarding expression, biophysical properties, and physiological impact of voltage-dependent sodium channels (Black et al., 1996; Catterall et al., 2005; Rush et al., 2007; Cummins et al., 2007; Fukuoka et al., 2008; Docherty and Farmer, 2009; Dib-Hajj et al., 2010). Generally speaking, these neurons are classified into three groups based on cell body diameter and their corresponding conduction velocities (Harper and Lawson, 1985a,b; Lawson, 2002). Small diameter neurons (<25 $\mu$m) give rise to unmyelinated C-fibers, which have slow conduction velocities (<1.4 m/s), medium diameter neurons (25–40 $\mu$m) give rise to lightly myelinated A$\delta$ fibers having faster conduction velocities (2–8 m/s), and large diameter neurons (>40 $\mu$m) give rise to more heavily myelinated A$\alpha/\beta$ fibers that have conduction velocities >14 m/s (Harper and Lawson, 1985a,b; Lawson, 2002). Previous studies (Black et al., 1996; Cummins et al., 2007; Fukuoka et al., 2008; Docherty and Farmer, 2009; Dib-Hajj et al., 2010) have shown that sensory neurons in the rat DRG express the TTX-sensitive sodium channels Nav1.1, Nav1.2, Nav1.3, Nav1.6, and Nav1.7 as well as the TTX-resistant channels Nav1.5, Nav1.8, and Nav1.9. Nav1.1 and Nav1.6 are preferentially expressed in large diameter (>50 $\mu$m) sensory neurons, although these subtypes are expressed at low levels in small and medium diameter sensory neurons. Nav1.2 and Nav1.5 appear to be expressed at low levels in nociceptive small diameter (<25 $\mu$m) sensory neurons. The small diameter neurons are of particular interest as they are often the predominant cell type involved in painful or nociceptive signaling. It is important to consider that some portion of the total expression for individual sodium channel subtypes may be contributed from glia localized in DRG as previous studies have documented expression of

Please cite this article in press as: Hodgdon KE, et al., Dorsal root ganglia isolated from *Nf1*+/− mice exhibit increased levels of mRNA expression of . . . , Neuroscience (2012), doi: 10.1016/j.neuroscience.2011.12.045

ARTICLE IN PRESS



sodium channels in both astrocytes and microglia (Bevan et al., 1985; Waxman et al., 1993; Black et al., 2009, 2010).

Our observations are consistent with recent reports examining the expression of sodium channel subtypes in rat sensory neurons. Using mRNA isolated from rat L4/5 DRG, Berta et al. (2008) found that Nav1.7 was the most abundant transcript, Nav1.8 and Nav1.6 were about half the levels of Nav1.7 and Nav1.1 was slightly less than Nav1.6. The levels of Nav1.2, Nav1.3, and Nav1.9 were much lower and Nav1.5 was undetected. For the $\beta$ subunits, $\beta$1 and $\beta$4 were about equal, whereas $\beta$3 and $\beta$2 were much less expressed. The expression profiles of Nav1.9 and the $\beta$ subunits are different than what we report in mouse sensory neurons; however, we obtained mRNA from L4/5 as well as more rostral DRG. In sensory neurons isolated from the L4/5 DRG of adult rats and grown in culture for $<$30 h, Nav1.7 exhibited the highest level of expression with Nav1.8 and Nav1.1 being the next most abundant, Nav1.2, Nav1.3, and Nav1.6 were substantially less (Wang et al., 2008). The level of Nav1.9 was quite low in the isolated neurons, although Nav1.9 was comparable with Nav1.8 in the intact whole DRG, which is in contrast to the findings reported by Berta et al. Nav1.4 and Nav1.5 were not detected by these authors. In electrophysiologically characterized rat sensory neurons that underwent single cell qPCR (Ho and O'Leary, 2011), Nav1.7, Nav1.8, and Nav1.9 were the most prominently expressed subtypes in small diameter ($<$25 $\mu$m) sensory neurons, although Nav1.1, Nav1.2, and Nav1.6 were detected at lower levels. In large diameter ($>$30 $\mu$m) neurons, Nav1.7 was the most abundant followed by Nav1.6 and Nav1.1, with only low levels of Nav1.2 and Nav1.9 detected. A surprisingly high expression of Nav1.8 was exhibited by a subpopulation of large neurons. Nav1.5 was detected in approximately 14% of the neurons examined (Ho and O'Leary, 2011). In contrast to findings obtained in rat DRG, we found that the fractional expression of Nav1.9 was the highest of all the $\alpha$ subunits in the mouse DRG. Previous results indicated that Nav1.9 was expressed in only $\sim$50% of rat unmyelinated C-fibers (Amaya et al., 2000; Fukuoka et al., 2008). However, using the average number of mRNA copies measured in single sensory neurons isolated from rat DRG as reported by Ho and O'Leary (2011), the fractional expression of Nav1.9 in small diameter ($<$25 $\mu$m) neurons was $\sim$35% of the total ($n$=70 neurons), whereas in the large diameter ($>$30 $\mu$m) it was only $\sim$5% ($n$=69 neurons) (O'Leary, personal communication). In addition, in whole isolated rat ganglia, Nav1.9 comprised $\sim$28$\pm$2% of the total mRNA ($n$=4 ganglia) and is similar to our value for Nav1.9 making up $\sim$40% of the total mRNA (O'Leary, personal communication). The exact origins for the differences reported in the literature are presently unknown. To our knowledge, our study is the first to quantitatively determine the expression levels for Nav subunits in mouse DRG; hence, one possibility for the larger expression of Nav1.9 mRNA is a species difference between rat and mouse. It is also possible that in the mouse DRG there may be large amounts of Nav1.9 mRNA held in reserve for translational upon metabolic demands or after neuronal injury. This is a subject for further investigation.

Nav1.7 is the predominant TTX-sensitive sodium channel expressed in small diameter neurons where it may play an important role in action potential firing. The slowly developing inactivation properties of Nav1.7 promote action potential generation in response to slow depolarizing stimuli (Cummins et al., 1998). Therefore, it is likely that the near twofold increase in Nav1.7 expression seen in the *Nf1*+/− neurons would play a significant role in mediating the increased sodium current density and increased excitability that we have observed in the *Nf1*+/− sensory neurons compared with those from wildtype mice (Wang et al., 2005, 2010). Although Nav1.7 appears to be the highest expressed TTX-sensitive $\alpha$ subunit based on mRNA levels in small diameter sensory neurons, the amplitude of compound action potentials measured from sciatic C-fibers in Scn8 *med* mice (Nav1.6 knock-out) was diminished, suggesting that Nav1.6 does contribute to action potential generation in these unmyelinated fibers (Black et al., 2002). Nav1.8 and Nav1.9 are the predominant TTX-resistant channels in small diameter neurons wherein Nav1.8 is thought to contribute to setting the firing threshold and regulating the upstroke of the action potential (Renganathan et al., 2001; Blair and Bean, 2002), whereas Nav1.9 may give rise to a persistent sodium current that influences excitability as well as in setting the resting membrane potential (Cummins et al., 1999; Herzog et al., 2001; Baker et al., 2003). However, at the normal resting potential of sensory neurons (around −60 mV), Nav1.9 is 97% inactivated by ultra-slow inactivation such that this channel subtype may contribute little, if any, to the normal excitability of these neurons (Cummins et al., 1999). Of the TTX-resistant channels in sensory neurons, expression of Nav1.8 was significantly elevated in the *Nf1*+/−DRG compared with wildtype, suggesting that an increase in this channel is responsible for a component of the increased excitability of *Nf1*+/− sensory neurons at resting membrane potentials. TTX-resistant subtypes have been detected in large diameter neurons; however, the functional role of these channels in the physiological response of large diameter neurons is not presently understood. Interestingly, Nav1.3 is expressed in embryonic sensory neurons and then in adulthood this subtype is greatly diminished (Waxman et al., 1994; Dib-Hajj et al., 1996; Felts et al., 1997). After nerve injury Nav1.3 is re-expressed and may contribute to the increased excitability observed after injury (Cummins and Waxman, 1997; Cummins et al., 2001). Based on this, it is possible that the enhanced excitability and TTX-sensitive sodium current density observed in *Nf1*+/− sensory neurons could result from the increased expression of Nav1.3; however, this seems unlikely because Nav1.3 makes up only a small fraction of the total complement of sodium channel (Fig. 2A). Despite the significant increases in the dominant channels, Nav1.7 and 1.8, are much more likely to be driving the changes in sodium current densities and excitability observed in *Nf1*+/− sensory neurons. Because gain of function mutations or increased expression of Nav1.7 or increased expression of Nav1.8 are associ-

Please cite this article in press as: Hodgdon KE, et al., Dorsal root ganglia isolated from *Nf1*+/− mice exhibit increased levels of mRNA expression of . . . , Neuroscience (2012), doi: 10.1016/j.neuroscience.2011.12.045

ARTICLE IN PRESS



ated with increased pain in humans (Jarecki et al., 2008, 2010; Cregg et al., 2010; Dib-Hajj et al., 2010), increases in the expression of these channels in those with NF1 may play a role in the increased intensity of sensory symptoms experienced by some with this disorder. The causal mechanisms that give rise to changes in sodium channel gene expression in the context of reduced neurofibromin and the corresponding chronic enhancement of Ras activity are unexplored. Acute inhibition of Ras activation by the Ras blocking antibody, Y13-259, did not restore the increased excitability of *Nf1*+/− sensory neurons (Duan et al., 2011) back to levels observed in wildtype sensory neurons. This result indicates that it is the long-term reduction in neurofibromin, through increased Ras signaling that is responsible for the increased sodium channel expression and excitability in *Nf1*+/− sensory neurons. As inhibition of Ras did not recapitulate the lower levels of neuronal excitability observed in wildtype neurons, this would suggest that acute post-translational modifications of Nav do not contribute to the increased sodium current densities; however, it is possible that other cellular mechanisms downstream of Ras may regulate membrane currents. These potential mechanisms remain an area of active investigation. Although the origins by which NF1 causes enhanced painful sensation have not been elucidated, it is likely that these abnormal painful states involve the sensitization of small diameter nociceptive sensory neurons and may underlie the onset of enhanced painful sensation in people with NF1.

In conclusion, in the DRG isolated from wildtype mice, the Nav1.9 subtype was the most abundant with Nav1.7 and Nav1.8 being the next most abundant subtypes. For the auxiliary $\beta$ subunits, $\beta$1 was by far the most abundant subtype. The mRNA for the $\alpha$ subunits of the sodium channels Nav1.1, Nav1.3, Nav1.7, and Nav1.8 were significantly elevated in DRG isolated from *Nf1*+/− mice. There were no significant changes in the relative expression levels of the auxiliary $\beta$ subunits. These results suggest that increased expression levels of Nav1.7, Nav1.8, and perhaps Nav1.1 in the *Nf1*+/−DRG make the largest contribution to the increased sodium current density and thus give rise to the enhanced excitability.

*Acknowledgments—This investigation was conducted in a facility constructed with support from Research Facilities Improvement Program grant Number C06 RR015481-01 from the National Center for Research Resources, NIH. This work was supported by awards from NIH NINDS NS51668 (C.M.H.) and the Department of Defense number W81XWH-09-1-0174 (G.D.N.).*

## REFERENCES

Amaya F, Decosterd I, Samad TA, Plumpton C, Tate S, Mannion RJ, Costigan M, Woolf CJ (2000) Diversity of expression of the sensory neuron-specific TTX-resistant voltage-gated sodium ion channels SNS and SNS2. Mol Cell Neurosci 15:331–342.

Baker MD, Chandra SY, Ding Y, Waxman SG, Wood JN (2003) GTP-induced tetrodotoxin-resistant Na+ current regulates excitability in mouse and rat small diameter sensory neurones. J Physiol 548: 373–382.

Berta T, Poirot O, Pertin M, Ji RR, Kellenberger S, Decosterd I (2008) Transcriptional and functional profiles of voltage-gated Na(+) channels in injured and non-injured DRG neurons in the SNI model of neuropathic pain. Mol Cell Neurosci 37:196–208.

Bevan S, Chiu SY, Gray PT, Ritchie JM (1985) The presence of voltage-gated sodium, potassium and chloride channels in rat cultured astrocytes. Proc R Soc Lond B Biol Sci 225:299–313.

Black JA, Dib-Hajj S, McNabola K, Jeste S, Rizzo MA, Kocsis JD, Waxman SG (1996) Spinal sensory neurons express multiple sodium channel alpha-subunit mRNAs. Brain Res Mol Brain Res 43:117–131.

Black JA, Liu S, Waxman SG (2009) Sodium channel activity modulates multiple functions in microglia. Glia 57:1072–1081.

Black JA, Newcombe J, Waxman SG (2010) Astrocytes within multiple sclerosis lesions upregulate sodium channel Nav1.5. Brain 133: 835–846.

Black JA, Renganathan M, Waxman SG (2002) Sodium channel Na(v)1.6 is expressed along nonmyelinated axons and it contributes to conduction. Brain Res Mol Brain Res 105:19–28.

Blair NT, Bean BP (2002) Roles of tetrodotoxin (TTX)-sensitive Na+ current, TTX-resistant Na+ current, and Ca2+ current in the action potentials of nociceptive sensory neurons. J Neurosci 22:10277–10290.

Catterall WA, Goldin AL, Waxman SG (2005) International Union of Pharmacology. XLVII. Nomenclature and structure-function relationships of voltage-gated sodium channels. Pharmacol Rev 57: 397–409.

Créange A, Zeller J, Rostaing-Rigattieri S, Brugières P, Degos JD, Revuz J, Wolkenstein P (1999) Neurological complications of neurofibromatosis type 1 in adulthood. Brain 122:473–481.

Cregg R, Momin A, Rugiero F, Wood JN, Zhao J (2010) Pain channelopathies. J Physiol 588:1897–1904.

Cummins TR, Aglieco F, Renganathan M, Herzog RI, Dib-Hajj SD, Waxman SG (2001) Nav1. 3 sodium channels: rapid repriming and slow closed-state inactivation display quantitative differences after expression in a mammalian cell line and in spinal sensory neurons. J Neurosci 21:5952–5961.

Cummins TR, Dib-Hajj SD, Black JA, Akopian AN, Wood JN, Waxman SG (1999) A novel persistent tetrodotoxin-resistant sodium current in SNS-null and wild-type small primary sensory neurons. J Neurosci 19:RC43.

Cummins TR, Howe JR, Waxman SG (1998) Slow closed-state inactivation: a novel mechanism underlying ramp currents in cells expressing the hNE/PN1 sodium channel. J Neurosci 18:9607–9619.

Cummins TR, Sheets PL, Waxman SG (2007) The roles of sodium channels in nociception: implications for mechanisms of pain. Pain 131:243–257.

Cummins TR, Waxman SG (1997) Downregulation of tetrodotoxin-resistant sodium currents and upregulation of a rapidly repriming tetrodotoxin-sensitive sodium current in small spinal sensory neurons after nerve injury. J Neurosci 17:3503–3514.

Daston MM, Scrable H, Nordlund M, Sturbaum AK, Nissen LM, Ratner N (1992) The protein product of the neurofibromatosis type 1 gene is expressed at highest abundance in neurons, Schwann cells, and oligodendrocytes. Neuron 8:415–428.

Dib-Hajj S, Black JA, Felts P, Waxman SG (1996) Down-regulation of transcripts for Na channel alpha-SNS in spinal sensory neurons following axotomy. Proc Natl Acad Sci U S A 93:14950–14954.

Dib-Hajj SD, Cummins TR, Black JA, Waxman SG (2010) Sodium channels in normal and pathological pain. Annu Rev Neurosci 33: 325–347.

Docherty RJ, Farmer CE (2009) The pharmacology of voltage-gated sodium channels in sensory neurones. Handb Exp Pharmacol 194:519–561.

Duan JH, Wang Y, Duarte D, Vasko MR, Nicol GD, Hingtgen CM (2011) Ras signaling pathways mediate NGF-induced enhancement of excitability of small-diameter capsaicin-sensitive sensory

Please cite this article in press as: Hodgdon KE, et al., Dorsal root ganglia isolated from *Nf1*+/− mice exhibit increased levels of mRNA expression of . . . , Neuroscience (2012), doi: 10.1016/j.neuroscience.2011.12.045

ARTICLE IN PRESS



neurons from wildtype but not Nf1+/− mice. Neurosci Lett 496: 70–74.

Felts PA, Yokoyama S, Dib-Hajj S, Black JA, Waxman SG (1997) Sodium channel alpha-subunit mRNAs I, II, III, NaG, Na6 and hNE (PN1): different expression patterns in developing rat nervous system. Brain Res Mol Brain Res 45:71–82.

Friedman JM (1999) Epidemiology of neurofibromatosis type 1. Am J Med Genet 89:1–6.

Fukuoka T, Kobayashi K, Yamanaka H, Obata K, Dai Y, Noguchi K (2008) Comparative study of the distribution of the alpha-subunits of voltage-gated sodium channels in normal and axotomized rat dorsal root ganglion neurons. J Comp Neurol 510:188–206.

Goldin AL (2001) Resurgence of sodium channel research. Annu Rev Physiol 63:871–894.

Harper AA, Lawson SN (1985a) Conduction velocity is related to morphological cell type in rat dorsal root ganglion neurones. J Physiol 359:31–46.

Harper AA, Lawson SN (1985b) Electrical properties of rat dorsal root ganglion neurones with different peripheral nerve conduction velocities. J Physiol 359:47–63.

Hemmick LM, Perney TM, Flamm RE, Kaczmarek LK, Birnberg NC (1992) Expression of the H-ras oncogene induces potassium conductance and neuron-specific potassium channel mRNAs in the AtT20 cell line. J Neurosci 12:2007–2014.

Herzog RI, Cummins TR, Waxman SG (2001) Persistent TTX-resistant Na+ current affects resting potential and response to depolarization in simulated spinal sensory neurons. J Neurophysiol 86:1351–1364.

Ho C, O'Leary ME (2011) Single-cell analysis of sodium channel expression in dorsal root ganglion neurons. Mol Cell Neurosci 46:159–166.

Isom LL (2001) Sodium channel beta subunits: anything but auxiliary. Neuroscientist 7:42–54.

Jacks T, Shih TS, Schmitt EM, Bronson RT, Bernards A, Weinberg RA (1994) Tumour predisposition in mice heterozygous for a targeted mutation in Nf1. Nat Genet 7:353–361.

Jarecki BW, Piekarz AD, Jackson JO 2nd, Cummins TR (2010) Human voltage-gated sodium channel mutations that cause inherited neuronal and muscle channelopathies increase resurgent sodium currents. J Clin Invest 120:369–378.

Jarecki BW, Sheets PL, Jackson JO 2nd, Cummins TR (2008) Paroxysmal extreme pain disorder mutations within the D3/S4-S5 linker of Nav1.7 cause moderate destabilization of fast inactivation. J Physiol 586:4137–4153.

Largaespada DA, Brannan CI, Jenkins NA, Copeland NG (1996) Nf1 deficiency causes Ras-mediated granulocyte/macrophage colony stimulating factor hypersensitivity and chronic myeloid leukaemia. Nat Genet 12:137–143.

Lau NB, Feldkamp MM, Roncari L, Loehr AH, Shannon P, Gutmann DH, Guha A (2000) Loss of neurofibromin is associated with activation of RAS/MAPK and PI3-K/AKT signaling in a neurofibromatosis 1 astrocytoma. J Neuropathol Exp Neurol 59:759–767.

Lawson SN (2002) Phenotype and function of somatic primary afferent nociceptive neurones with C-, Aδ or Aα/β-fibres. Exp Physiol 87:239–244.

Patino GA, Isom LL (2010) Electrophysiology and beyond: multiple roles of Na+ channel β subunits in development and disease. Neurosci Lett 486:53–59.

Pfaffl MW (2001) A new mathematical model for relative quantification in real-time RT-PCR. Nucleic Acids Res 29:e45.

Pfaffl MW, Horgan GW, Dempfle L (2002) Relative expression software tool (REST) for group-wise comparison and statistical analysis of relative expression results in real-time PCR. Nucleic Acids Res 30:e36.

Rane SG (1991) A Ca2(+)-activated K+ current in ras-transformed fibroblasts is absent from nontransformed cells. Am J Physiol 260:C104–C112.

Renganathan M, Cummins TR, Waxman SG (2001) Contribution of Na(v)1.8 sodium channels to action potential electrogenesis in DRG neurons. J Neurophysiol 86:629–640.

Rogart RB, Cribbs LL, Muglia LK, Kephart DD, Kaiser MW (1989) Molecular cloning of a putative tetrodotoxin-resistant rat heart Na+ channel isoform. Proc Natl Acad Sci U S A 86:8170–8174.

Rush AM, Cummins TR, Waxman SG (2007) Multiple sodium channels and their roles in electrogenesis within dorsal root ganglion neurons. J Physiol 579:1–14.

Trimmer JS, Cooperman SS, Tomiko SA, Zhou JY, Crean SM, Boyle MB, Kallen RG, Sheng ZH, Barchi RL, Sigworth FJ et al. (1989) Primary structure and functional expression of a mammalian skeletal muscle sodium channel. Neuron 3:33–49.

Vogel KS, Brannan CI, Jenkins NA, Copeland NG, Parada LF (1995) Loss of neurofibromin results in neurotrophin-independent survival of embryonic sensory and sympathetic neurons. Cell 82:733–742.

Wang JG, Strong JA, Xie W, Yang RH, Coyle DE, Wick DM, Dorsey ED, Zhang JM (2008) The chemokine CXCL1/growth related oncogene increases sodium currents and neuronal excitability in small diameter sensory neurons. Mol Pain 4:38.

Wang Y, Duan JH, Hingtgen CM, Nicol GD (2010) Augmented sodium currents contribute to the enhanced excitability of small diameter capsaicin-sensitive sensory neurons isolated from Nf1+/−mice. J Neurophysiol 103:2085–2094.

Wang Y, Nicol GD, Clapp DW, Hingtgen CM (2005) Sensory neurons from Nf1 haploinsufficient mice exhibit increased excitability. J Neurophysiol 94:3670–3676.

Waxman SG, Kocsis JD, Black JA (1994) Type III sodium channel mRNA is expressed in embryonic but not adult spinal sensory neurons, and is reexpressed following axotomy. J Neurophysiol 72:466–470.

Waxman SG, Sontheimer H, Black JA, Minturn JE, Ransom BR (1993) Dynamic aspects of sodium channel expression in astrocytes. Adv Neurol 59:135–155.

Wolkenstein P, Zeller J, Revuz J, Ecosse E, Leplège A (2001) Quality-of-life impairment in neurofibromatosis type 1: a cross-sectional study of 128 cases. Arch Dermatol 137:1421–1425.

Zhang YY, Vik TA, Ryder JW, Srour EF, Jacks T, Shannon K, Clapp DW (1998) Nf1 regulates hematopoietic progenitor cell growth and ras signaling in response to multiple cytokines. J Exp Med 187: 1893–1902.

*(Accepted 23 December 2011)*

Please cite this article in press as: Hodgdon KE, et al., Dorsal root ganglia isolated from *Nf1*+/− mice exhibit increased levels of mRNA expression of . . . , Neuroscience (2012), doi: 10.1016/j.neuroscience.2011.12.045